VIP blockade leads to microcephaly in mice via disruption of Mcph1-Chk1 signaling

Sandrine Passemard,[1,2,3,4] Vincent El Ghouzzi,[1,2] Hala Nasser,[1,2] Catherine Verney,[1,2] Guilan Vodjdani,[5] Adrien Lacaud,[6,7] Sophie Lebon,[1,2] Marc Laburthe,[2,8] Patrick Robberecht,[9] Jeannette Nardelli,[1,2] Shyamala Mani,[10] Alain Verloes,[1,2,4] Pierre Gressens,[1,2,3,11] and Vincent Lelièvre[1,2,6,7]

[1]Inserm, U676, Paris, France. [2]Université Paris 7, Faculté de Médecine Denis Diderot, Paris, France. [3]Assistance Publique Hôpitaux de Paris (AP HP), Hôpital Robert Debré, Service de Neurologie Pédiatrique, and [4]AP HP, Hôpital Robert Debré, Service de Génétique Clinique, Paris, France. [5]Centre de Recherche de l'Institut du Cerveau et de la Moelle épinière, CNRS UMR-7225, Inserm UMR-975, Université Pierre et Marie Curie, Paris, France. [6]CNRS, UPR 3212, Strasbourg, France. [7]Université de Strasbourg, Strasbourg, France. [8]Inserm, U773, Paris, France. [9]Laboratory of Biological Chemistry and Nutrition, Université Libre de Bruxelles, Brussels, Belgium. [10]Center for Neuroscience, Indian Institute of Science, Bangalore, India. [11]Centre for the Developing Brain, Imperial College, Hammersmith Campus, London, United Kingdom.

Autosomal recessive primary microcephaly (MCPH) is a genetic disorder that causes a reduction of cortical outgrowth without severe interference with cortical patterning. It is associated with mutations in a number of genes encoding protein involved in mitotic spindle formation and centrosomal activities or cell cycle control. We have shown previously that blocking vasoactive intestinal peptide (VIP) during gestation in mice by using a VIP antagonist (VA) results in microcephaly. Here, we have shown that the cortical abnormalities caused by prenatal VA administration mimic the phenotype described in MCPH patients and that VIP blockade during neurogenesis specifically disrupts Mcph1 signaling. VA administration reduced neuroepithelial progenitor proliferation by increasing cell cycle length and promoting cell cycle exit and premature neuronal differentiation. Quantitative RT-PCR and Western blot showed that VA downregulated Mcph1. Inhibition of Mcph1 expression led to downregulation of Chk1 and reduction of Chk1 kinase activity. The inhibition of Mcph1 and Chk1 affected the expression of a specific subset of cell cycle–controlling genes and turned off neural stem cell proliferation in neurospheres. Furthermore, in vitro silencing of either Mcph1 or Chk1 in neurospheres mimicked VA-induced inhibition of cell proliferation. These results demonstrate that VIP blockade induces microcephaly through Mcph1 signaling and suggest that VIP/Mcph1/Chk1 signaling is key for normal cortical development.

Introduction

Autosomal recessive primary microcephaly (MCPH) is a genetic affection often characterized by a severe reduction of brain size without cortical cytoarchitecture defect, as defined at birth by an occipital frontal circumference (OFC) below –2 SD or more from normal range (1). MCPH patients usually exhibit mild developmental delay associated with hyperkinesia and, most often, mild to severe cognitive impairment (2, 3). Seven genes are currently identified in MCPH-related patients, namely *BRIT1/MCPH1* (BRCT–repeat inhibitor of hTert expression, which encodes MICROCEPHALIN; locus MCPH1) (4), *WDR62* (WD repeat domain 62; MCPH2) (5–7), *CDK5RAP2* (cyclin-dependent kinase 5 regulatory associated protein 2; MCPH3) (8), *CEP152* (centrosomal protein 152 kDa; MCPH4) (9), *ASPM* (abnormal spindle-like microcephaly-associated protein; MCPH5) (10), *CENPJ* (centromeric protein J; MCPH6) (8), and *STIL/SIL* (SCL/TAL1 interrupting locus; MCPH7) (11). While mutation-induced loss of function triggers a reduction of cortical expansion in MCPH-related patients, native proteins were found involved in cell cycle/checkpoint control (*MCPH1* and *STIL*, refs. 12–15), and/or mitotic spindle dynamics (*MCPH1*, *WDR62*, *CDK5RAP2*, *CEP152*, *ASPM*, *CENPJ*, and *STIL*; refs. 8 and 16–18). In addition, *MCPH1*, *CEP152*, and *STIL* were also implicated in radiation-induced DNA repair, apoptosis, and cancer (12, 19–25). Downstream, Checkpoint kinase 1 (*CHK1*), a target for *MCPH1*, is known to control progression of the cell cycle at crucial phases including S phase and G_2/M transition (14, 15, 21, 22, 25).

Although animal models would be of great help in better understanding MCPH-linked mechanisms, very few of them displaying MCPH phenotype are available so far. Genetic invalidations of intrinsic factors (i.e., *Stil*, *Chk1*, breast cancer 1 [*Brca1*]) have been carried out in mice but resulted in lethal phenotypes in utero (19, 26, 27). Two *Mcph1* knockout mice were very recently described (28, 29). In the *Mcph1/Brit1* conditional invalidation driven by the β-*actin* promoter, mutant mice exhibit mitotic and meiotic recombination, DNA repair defects resulting in genomic instability, and infertility (28). However, the brain phenotype has not yet been reported. In the other model, which was generated by gene trapping leading to the deletion of the C-terminal BRCT domain of Mcph1, adult mice do not have detectable brain weight loss although no detailed neuropathology has been reported (29). In addition, about 1,200 genes were either upregulated or downregulated when compared with WT brain (29). Interestingly, the *Nde1*$^{-/-}$ mouse (*NUDE* in humans, encoding a microtubule organizing center–associated [MTOC-associated] protein) is the only published genetic mouse model with a developmental brain phenotype showing a significant reduction (around 20%) of the overall brain volume with a specific reduction of upper layers (30). However, loss of function of NUDE has not been reported in MCPH-related patients.

Authorship note: Pierre Gressens and Vincent Lelièvre contributed equally to this work.

Conflict of interest: The authors have declared that no conflict of interest exists.

Citation for this article: *J Clin Invest.* 2011;121(8):3072–3087. doi:10.1172/JCI43824.

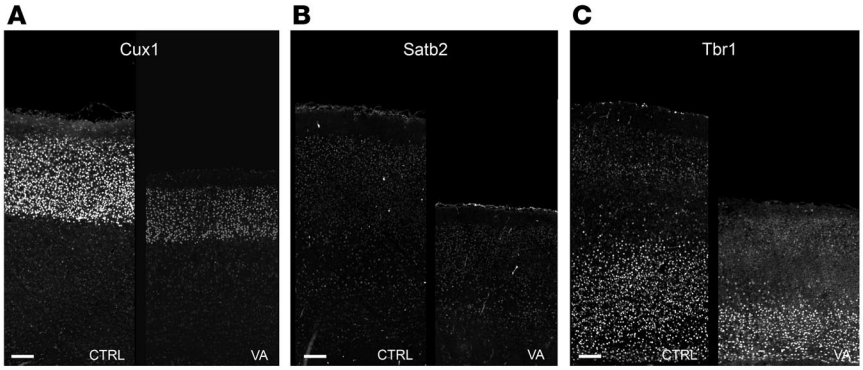

Figure 1
VIP blockade during neurogenesis induces microcephaly with thinner cortex and reduction of both upper and lower cortical layers. (**A**–**C**) Coronal P6 brain sections immunostained with specific markers of cortical layers (**A**: Cux1; **B**: Satb2; **C**: Tbr1) show that all layers are reduced in thickness in VA-treated animals when compared with age-matched controls (CTRL). Scale bars: 100 μm.

Developmental processes that are controlled by the MCPH loci may also depend on environmental factors. Deleterious extrinsic factors including alcohol, caffeine, morphine, and chemotherapeutic agents have been shown to modulate cell cycle duration and symmetrical versus asymmetrical divisions, resulting in limitations of the number of newborn cortical neurons (31–35). However, specific molecular targets of these extrinsic factors are not yet elucidated, except for ionizing radiation shown to have a negative impact on brain development by interfering with the ATR/CHK1/PCNT pathway (36). Conversely, beneficial extrinsic factors either produced by the embryo (including IGF-I and FGF10) or that cross the placenta barrier when produced by the mother (i.e., vitamin D3, thyroid hormone T3, NT3, or serotonin) can sustain boost or modulate embryonic brain development (37–40). Among these maternal factors, the vasoactive intestinal peptide (VIP) is produced in great amount during pregnancy (41) by lymphocytes present in decidual membranes (42) and elicits various neurotrophic actions including a major growth factor effect on embryogenesis, as shown previously on whole embryos treated ex utero with VIP (43). To date, none of these extracellular factors have been clearly connected with this ubiquitous machinery that dictates the appropriate number of neurons necessary to ensure the normal brain functions.

In line with these data, in the early 1990s, Gressens and coworkers described a pharmacologically induced murine model of microcephaly (44). In the latter, maternal VIP was challenged by a well-characterized VIP antagonist (VA) (45–47), which, when injected into pregnant females during neurogenesis (E9–E11), led to cortical alterations of newborn pups. These alterations involve the size but not the architecture of the cortex, a phenotype reminiscent of MCPH features in humans. Follow-up studies by the same investigators have suggested that VIP action on embryonic cortical expansion was related to a reduction of cell cycle duration including a shortening of the S phase (48). Nevertheless, at that time, no molecular mechanism was offered to explain such a drastic phenotype.

In the present study, we used this animal model and sought after the possible mechanism by which extrinsic factors such as VIP control cell cycle duration. To address this issue, we aimed to correlate VA-induced alteration of the VIP signaling pathway with modulation of expression of MCPH genes and their functions both in vivo and in vitro using embryos, newborn mice, and neurosphere-derived progenitors. We demonstrate that VIP blockade specifically downregulates *Mcph1-Chk1* expression and function, ultimately leading to cortical abnormalities that closely mimic features described in MCPH patients.

Results

VIP blockade during neurogenesis induces microcephaly with thinner cortex. VIP blockade results in microcephaly in mice: however, the phenotype has not been described yet at the histological and morphometric levels. A global morphometric analysis of brains from P5 pups born from either VA- or PBS-injected dams was performed. VA brains showed a reduced weight as compared with controls at P5 and P10, without statistically significant body weight reduction (Supplemental Figure 1, A and B; supplemental material available online with this article; doi:10.1172/JCI43824DS1). On Nissl-stained sections, a clear qualitative shrinkage of cortical thickness was observed (Supplemental Figure 1, C and D).

On selected coronal rostral and caudal levels of the primary somatosensory cortex (S1) (see Supplemental Methods), cortical surface (Supplemental Figure 1E) and thickness (Supplemental Figure 1F) were decreased in VA-treated animals as compared with controls. The cortical layers were thinner in VA than in controls, but differences were slightly bigger in rostral than in caudal somatosensory areas (i.e., 19%: 789 ± 92 μm vs. 645 ± 68 μm and 17%: 974 ± 63 μm vs. 775 ± 55 μm, respectively, n = per condition) (Supplemental Figure 1G).

The cortical neuronal density, assessed at the rostral level in the primary somatosensory cortex, did not reveal any significant difference in the number of neuronal nuclei–labeled (NeuN-labeled) neurons per surface unit between VA and controls (8180 ± 1085 cells/μm^2, n = 3; control, 8780 ± 778 cells/μm_2, n = 4) (Supplemental Figure 1H). However, measurement of the thickness of the superficial cortical layers (II–III–IV) versus deeper layers (V–VI) revealed a reduction of both the superficial and deep layers' thickness (Supplemental Figure 1, G and H). The use of specific

Table 1
VA lengthens cell cycle in dorsal telencephalic VZ progenitors of E11.5 embryos

Dorsal E11.5	Ts (h)[A]	Tc (h)[B]	Ts/Tc
Control	5.4 ± 0.38	12 ± 0.76	0.45 ± 0.02
VA	8.5 ± 0.87	29 ± 4	0.30 ± 0.02
P value (unpaired t test)	0.0317	0.0159	0.0159

Cell cycle parameters (mean ± SEM) calculated from IdU/BrdU double labeling (cf. Figure 2, C and D) according to ref. 49. [A]Length of S phase, Ts = Ti/(*Lcells*/*Scells*). [B]Total cell time, Tc = Ts/(*Scells*/*Pcells*). Ti, 1.5 hours; *Lcells*, IdU^+BrdU^-; *Scells*, IdU^+BrdU^+; *Pcells*, total number of proliferating cells, estimated by DAPI count in the VZ in the sampling area.

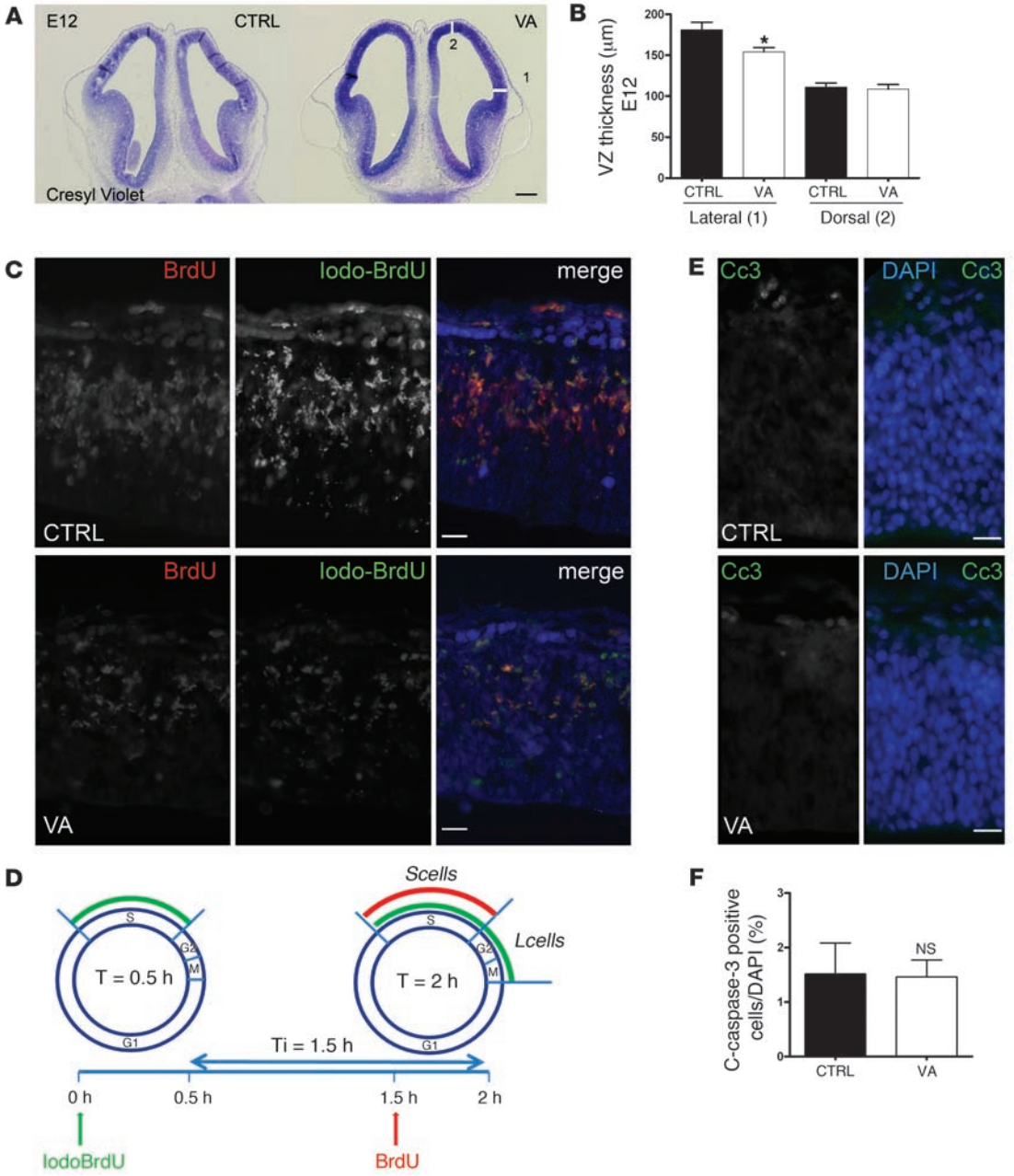

Figure 2

VA reduces cortical thickness in embryos by lengthening cell cycle during neurogenesis without inducing excess apoptosis. (**A**) Coronal section of control and VA brains from E12.5 embryos stained by cresyl violet. Scale bar: 200 μm. (**B**) Lateral and dorsal cortical thickness of E12.5 embryo telencephalon in control and VA groups ($n = 6$, unpaired t test, $^*P < 0.05$). (**C**) Double-labeling BrdU (red), IdU (green), and DAPI (blue) at E11.5 in the dorsal telencephalic VZ in control and VA sections. Scale bars: 20 μm. (**D**) Schematic representation of experimental BrdU-IdU procedure: injection at T0 hour with IdU and at T1.5 hour (Ti) with BrdU followed by sacrifice at T2.0 hour allows identification of the 3 cell types shown in **C**: those within the S phase at T0–T1.5 but within G_2/M at T1.5–T2.0 (labeled in green due to IdU-incorporation only = leaving fraction = *Lcells* = $IdU^+/BrdU^-$); cells entering S phase at T1.5–2.0 (labeled in red because of BrdU incorporation = $BrdU^+/IdU^-$); and finally cells within S phase at both T0 and T1.5 (labeled in yellow due to IdU/BrdU incorporation = S fraction = *Scells* = $IdU^+/BrdU^+$). DAPI counterstained nuclei in blue (*Pcells*). (**E** and **F**) Immunostaining for cleaved caspase-3 does not show any difference between control and VA-treated animals ($n = 8$ per group, t test, $^*P < 0.05$). Scale bars: 20 μm.

markers of cortical layers (Cut homeobox 1 [Cux1], expressed in layers II–IV, special AT-rich sequence-binding protein 2 [Satb2]; expressed by a subset of neurons throughout the cortical layers with a most prominent expression in layers II–IV; and T box brain 1 [Tbr1], expressed in layer VI) confirmed that all layers were affected by VA treatment (Figure 1). Astrocyte distribution appeared unchanged between groups as revealed by GFAP immunodetection (data not shown).

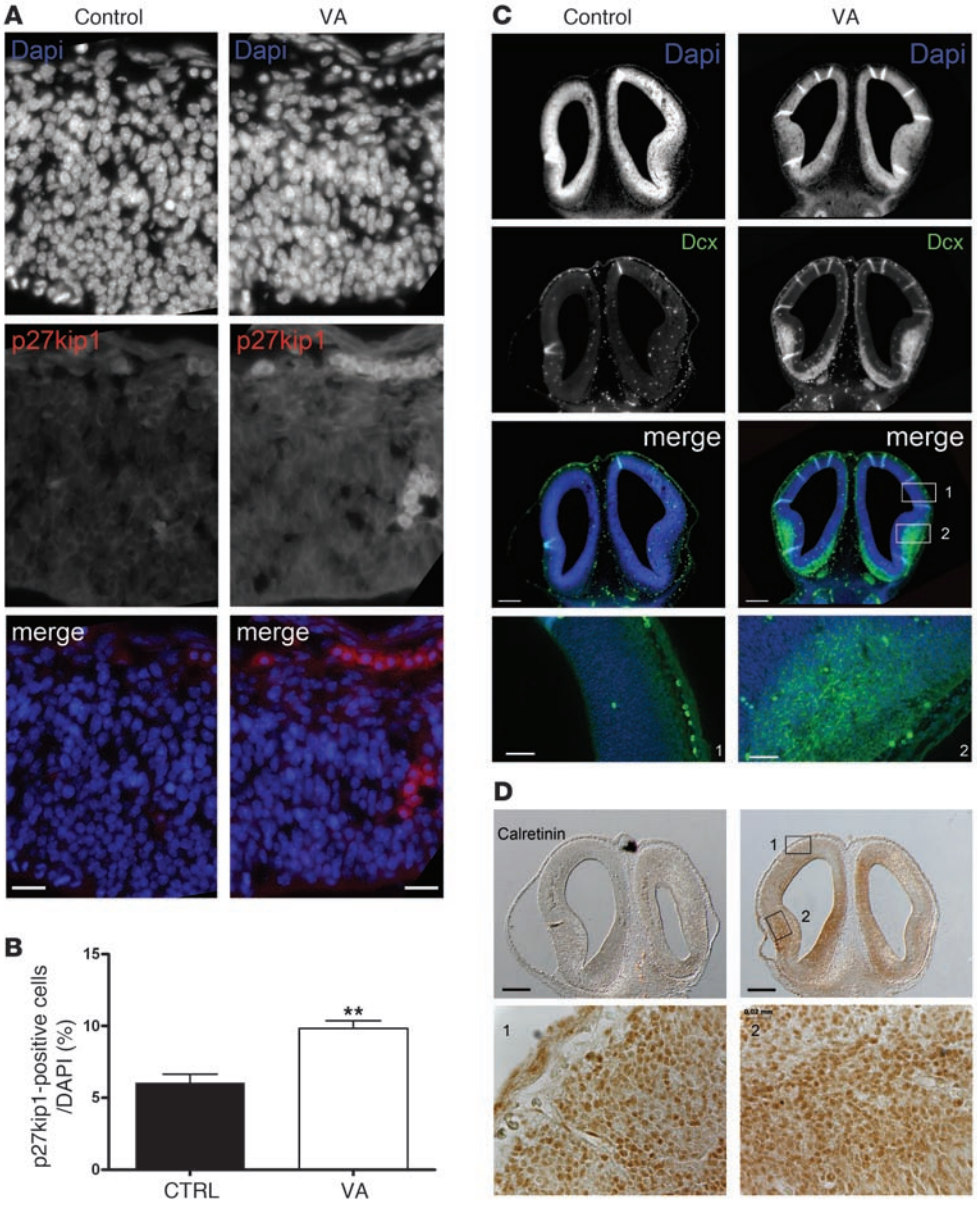

Figure 3

VA-induced microcephaly triggers cell cycle exit and early differentiation of cortical progenitors in embryos. (**A** and **B**) Immunofluorescent staining for p27kip1 on coronal E11.5 sections in dorsal telencephalon of VA-treated embryos compared with controls. Scale bars: 20 μm. The labeling index (number of p27kip1-positive cells over the total number of nuclei stained by DAPI) is increased in VA-treated embryos as compared with controls (n = 7 per group, unpaired t test, $^{**}P < 0.01$). (**C**) Immunofluorescent staining for Dcx on coronal E12.5 sections in dorsal telencephalon of VA-treated embryos compared with controls. Postmitotic Dcx-positive neurons are observed in VA-treated embryos in LGE and in the dorsal, medial, and lateral preplate, while positive staining remained almost absent in controls at E12.5. Scale bars: 200 μm). Lower panel shows high-magnification photographs of Dcx-immunoreactive cells in boxes 1 and 2. Scale bars: 50 μm. (**D**) Calretinin immunoreactivity at the same level as mentioned above. Note the intense labeling in LGE (box 2) and in the dorsal (box 1), medial, and lateral preplates, which are undetectable in controls. Scale bars: 200 μm. Lower panel shows high-magnification photographs of calretinin-immunoreactive cells in boxes 1 and 2.

Taken together, these data suggest that VIP blockade during early neurogenesis has a dramatic impact on cortical development.

VIP blockade decreases proliferation in neuroepithelial progenitors by increasing cell cycle length. To address whether VA could have a direct impact on neurogenesis, we analyzed proliferation and cell cycle length in embryos. Since the thickness reduction was already detectable as early as E12.5 in lateral telencephalic walls of VA-treated embryos (Figure 2, A and B), we analyzed progenitor proliferation 1 day before, i.e., in E11.5 VA-treated embryos and controls. To assess a potential decrease in cell proliferation, we first measured the cell cycle length in VA-treated and control telencephalic samples, using an elegant method previously described (49). Iododeoxyuridine (IdU) was injected into E11.5 pregnant females followed by BrdU (50 mg/g body weight each for both) 1.5 hours later. Dams were sacrificed 2 hours after the first injection (Figure 2D). As shown in Figure 2C and Supplemental Table 1, both BrdU and IdU labeling were reduced in VA animals. Cell cycle length calculation shown on Table 1 was performed by extracting the parameters S phase (Ts) and total cycle (Tc) durations as well as the Ts/Tc ratio from the number of positive cells for BrdU, IdU, or both. In line with previous studies (50, 51) performed in E11.5 ventricular zone (VZ) control brains, Ts was approximately 5.4 hours and Tc 12 hours. In VA-treated brains, both Ts and Tc were significantly lengthened: Ts approximately 8.5 hours and Tc approximately 29 hours, confirming that VA-induced VIP blockade between E9 and E11 reduces VZ progenitor proliferation by increasing the duration of both the S phase and the whole cell cycle.

At this stage, the number of apoptotic cells (cleaved caspase-3 and TUNEL positive) in the dorsal VZ was similar in VA and control telencephalon (Figure 2, E and F and data not shown).

VIP blockade accelerates cell cycle exit and leads to early differentiation of cortical progenitors. Since the reduction of VZ progenitors appeared secondary to the cell cycle lengthening in VA-treated telencephalon, we aimed to characterize the cell fate of these pro-

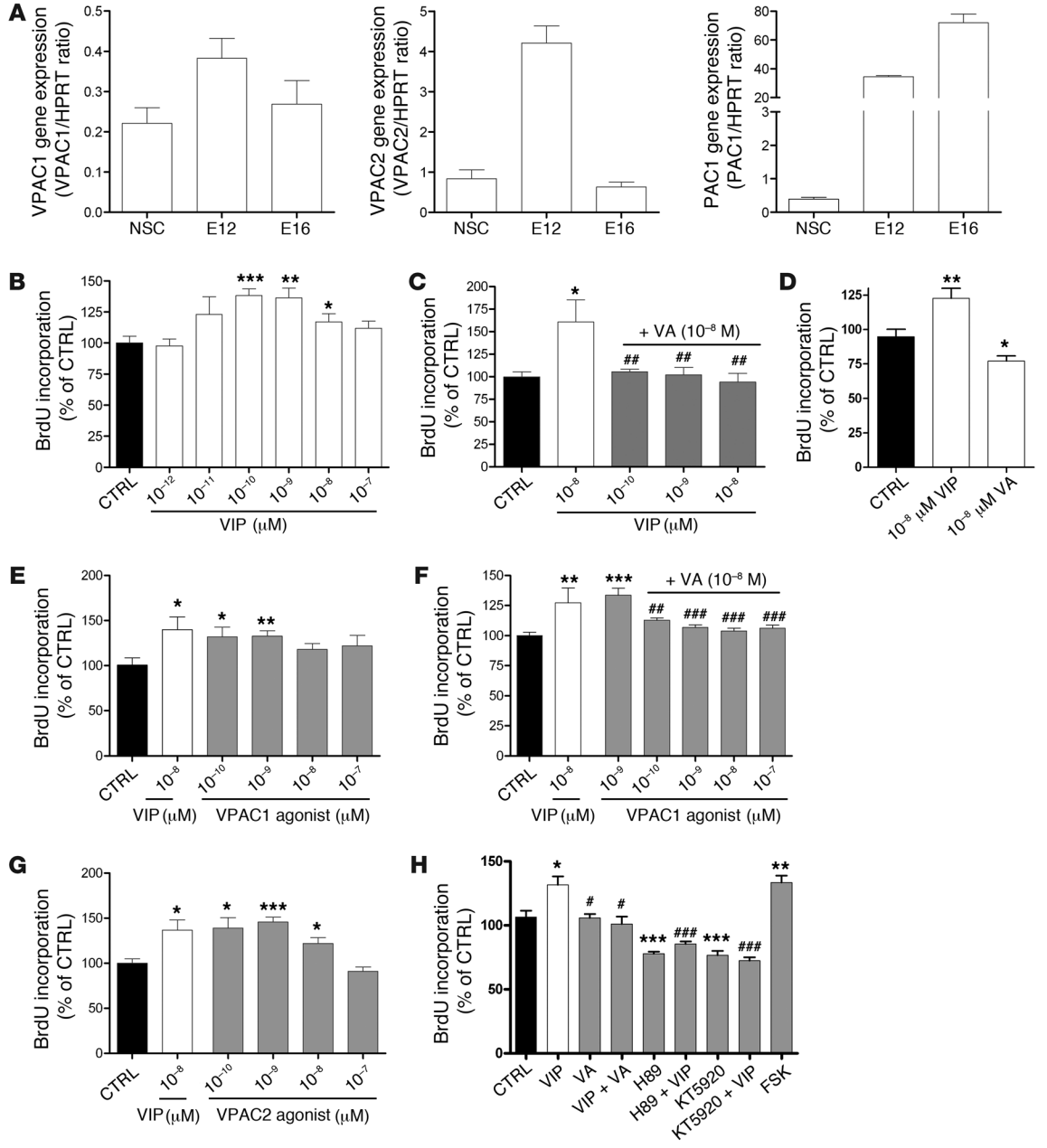

Figure 4

VA acts by interfering with VIP/VPAC signaling pathway and PKA activation. (**A**) VIP receptors and VPAC1 and VPAC2 expression levels as assessed by quantitative RT-PCR performed from neurosphere-derived progenitors and E12/E16 telencephalon. VPAC1 and VPAC2 receptors are mainly expressed in early stages, while PAC1 expression increased throughout the development. (**B**–**H**) BrdU incorporation assay performed on E10.5 neurosphere-derived progenitors. VIP stimulates proliferation of E10.5 neurosphere-derived progenitors in a dose-dependent manner (**B**). This effect is completely abrogated by VA at concentrations as low as 0.1 nM (**C**). VA alone decreases proliferation of neurosphere-derived progenitors compared with PBS (**D**). VPAC1 (**E** and **F**) and VPAC2 (**G**) agonists mimic VIP-induced BrdU incorporation. VIP stimulatory effect on BrdU incorporation is mimicked by the adenylate-cyclase activator FSK but is inhibited by H89 or KT5920, 2 separate inhibitors of PKA (**H**). ($n = 8$ per group, unpaired t test, $^{*}P < 0.05$, $^{**}P < 0.01$, or $^{***}P < 0.001$ between treatments and controls; or $^{\#}P < 0.05$, $^{\#\#}P < 0.01$, or $^{\#\#\#}P < 0.001$ between VIP and other treatments).

genitors. Therefore, we studied at E11.5 the expression pattern of p27kip1, a factor known to promote cell cycle exit of cortical progenitors (52). p27kip1-positive cells were highly increased in the dorsal telencephalon of VA-treated embryos as compared with age-matched controls, indicating that VIP blockade during early neurogenesis significantly promotes VZ progenitors to exit the cell cycle (Figure 3, A and B).

To investigate whether this loss of progenitors could influence the normal cell differentiation during early neurogenesis and corticogenesis phases, we assessed the doublecortin (Dcx) immu-

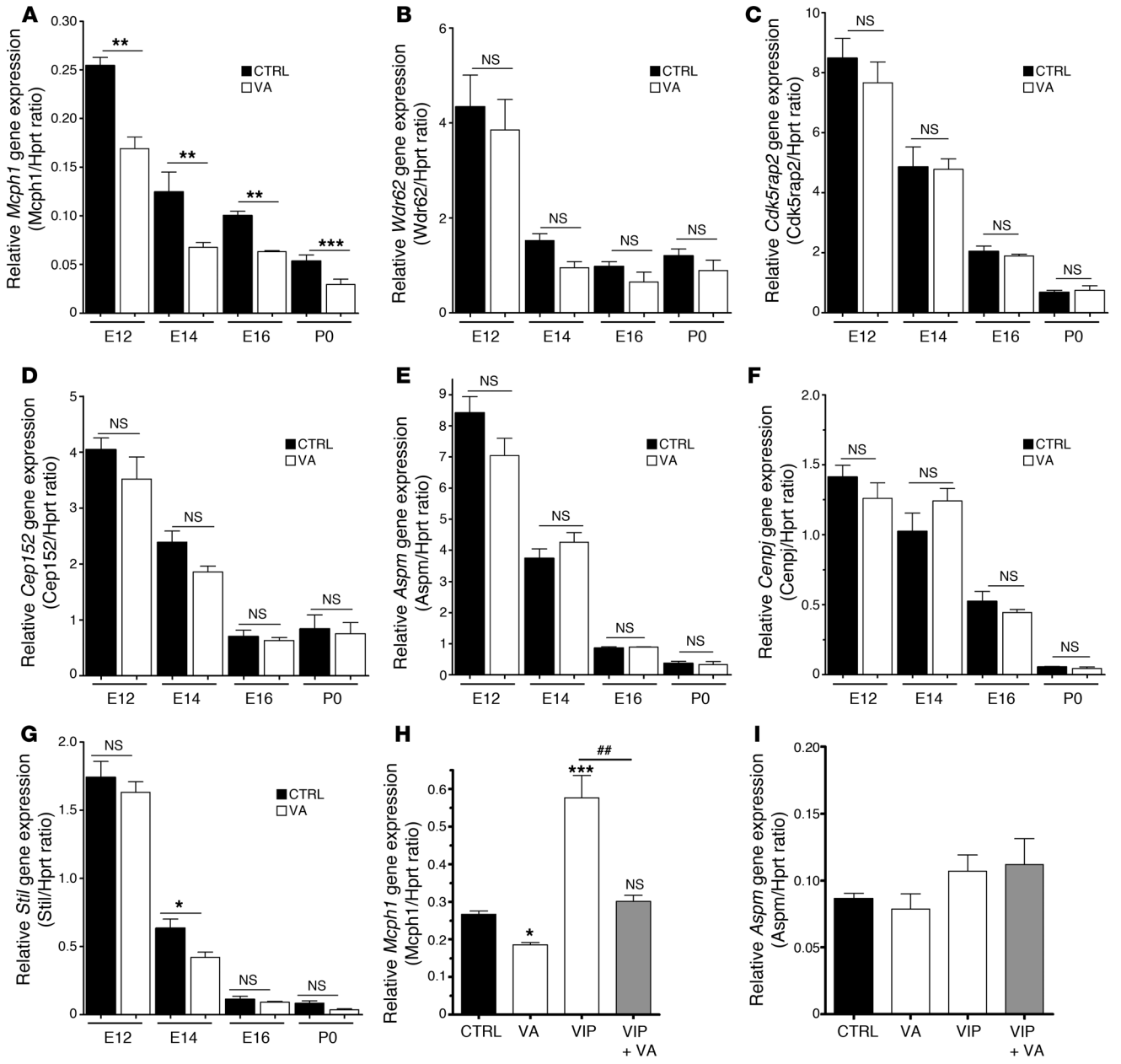

Figure 5

VA treatment affects specifically the expression of *Mcph1* genes in vivo. (**A**–**E**) Expression levels of all known *Mcph* genes: *Mcph1* (**A**), *Wdr62* (**B**), *Cdk5rap2* (**C**), *Cep152* (**D**), *Aspm* (**E**), *Cenpj* (**F**), and *Stil* (**G**) assessed by quantitative RT-PCR on RNA samples extracted from telencephalon of embryos (control or VA-treated) from E12 to P0. Parallel to the time-dependent reduction in *Mcph* gene expression, VA induced a significant decrease in *Mcph1* expression ($n = 8$, run in duplicate, 1-way ANOVA followed by Bonferroni's post-test, $^{*}P < 0.05$, $^{**}P < 0.01$, or $^{***}P < 0.001$) compared with controls (**A**). In contrast, no clear difference was observed between control and VA samples at the corresponding ages for *Wdr62*, *Cdk5rap2*, *Cep152*, *Aspm*, *Cenpj*, and *Stil* (**B**–**G**). (**H** and **I**) Rescue experiments performed on E16 telencephalic samples by quantitative RT-PCR. *Mcph1* transcription (**H**) is also upregulated by VIP ($^{*}P < 0.05$, $^{**}P < 0.01$, or $^{***}P < 0.001$), while coinjection of VA significantly represses VIP-induced overexpression ($^{\#}P < 0.05$, $^{\#\#}P < 0.01$, or $^{\#\#\#}P < 0.001$). *Aspm* expression used herein as negative control remains unaffected by VIP, VA, or both (**I**).

noreactivity in the telencephalon of E12 control and VA-treated embryos. Dcx is a microtubule-associated protein whose expression underlines mitosis exit and that is commonly used as an early marker of newborn postmitotic neurons (53). Dcx was expressed in VA-treated cortices with highest signals in lateral ganglionic eminence (LGE), while it remained undetectable in control cortices at this stage (Figure 3C). Similarly, immunostaining at E11.5 for Calretinin, a marker for Cajal-Retzius neurons, was not visible in controls while it strongly labeled VA-treated cortices (Figure 3D). Interestingly, Dcx- and Calretinin-positive postmitotic neurons were predominantly detected in the dorsal, lateral, and medial preplate and in LGE from VA-treated cortices (Figure 3, C and D).

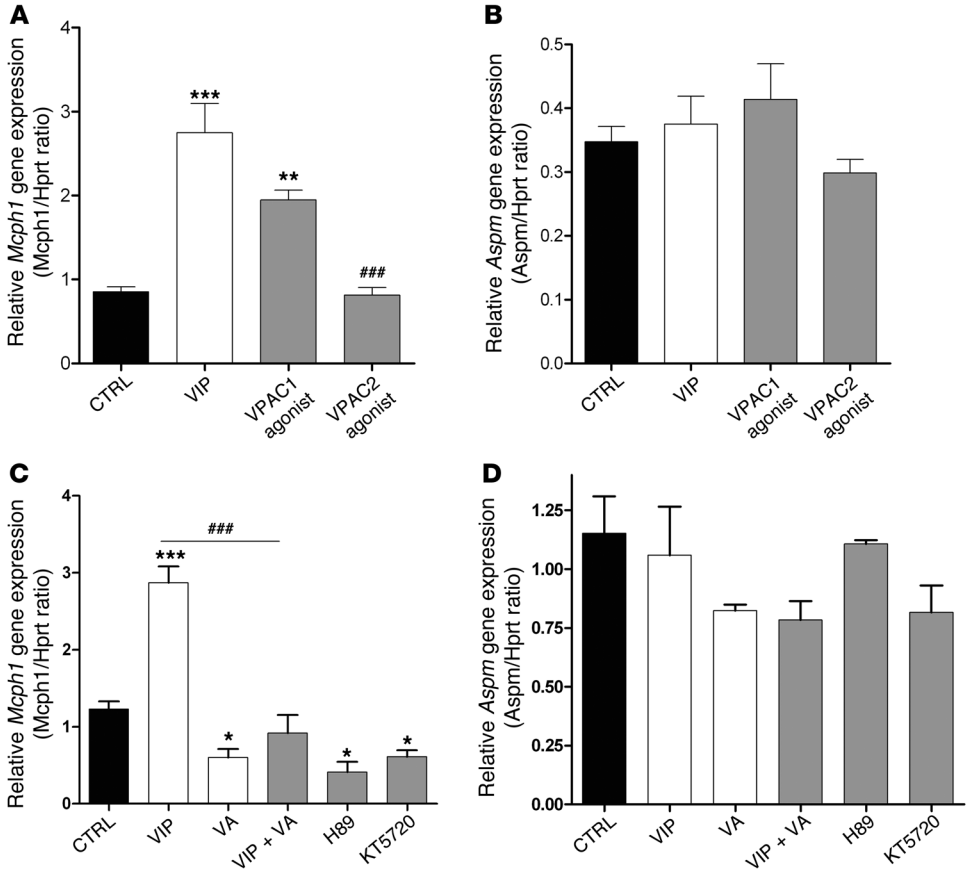

Figure 6
VA treatment affects *Mcph1* gene expression in E10.5 neurosphere-derived progenitors through VPAC1-PKA signaling. (**A** and **B**) *Mcph1* and *Aspm* (used as control) expression levels assessed by quantitative RT-PCR isolated from neurosphere cultures treated with VIP analogues. Note that only VPAC1 agonist was able to perfectly mimic VIP effects (n = 4 per group, run in duplicate, 1-way ANOVA, $^{*}P < 0.05$, $^{**}P < 0.01$, or $^{***}P < 0.001$). Once again, VPAC1 agonist failed to induce any change in *Aspm* expression. (**C** and **D**) Similar to the above experiment, neurosphere cultures were treated with VIP, VA, VIP plus VA, VIP plus H89 and KT5720, 2 PKA inhibitors, to analyze *Mcph1* or *Aspm* gene expression. VIP-induced stimulation of transcript levels (mean ± SEM) compared with controls (n = 4 per group, run in duplicate, 1-way ANOVA, $^{*}P < 0.05$, $^{**}P < 0.01$, or $^{***}P < 0.001$); VA reduces *Mcph1* transcript expression. VIP effects on *Mcph1* expression are abolished in the presence of VA ($^{\#\#}P < 0.01$, or $^{\#\#\#}P < 0.001$). 3 inhibitors of PKA reduce *Mcph1* expression, mimicking VA effects. *Aspm* gene expression was not modified by these treatments.

Together, our results indicate that VIP blockade during early neurogenesis promotes cell cycle exit and premature neuronal differentiation of VZ progenitors in both dorsal and ventral telencephalon without increased apoptosis.

VIP blockade inhibits the neurotrophic VIP signaling through cAMP-coupled VPAC receptors. To further dissect VIP signaling in our model, we first asked whether VIP receptors are expressed during neurogenesis. To this end, we measured the level of expression of the 3 known VIP and PACAP receptors (*Vpac1*, *Vpac2*, and *Pac1*) by quantitative PCR using RNA extracts from E12 and E16 embryonic forebrains and neurosphere-derived progenitors isolated from E10.5 forebrains. VIP and PACAP may actually interact with all 3 receptors, although VPAC2 and PAC1 are the predominant forms at these early stages of brain development. As shown in Figure 4A, *Vpac1*, *Vpac2*, and *Pac1* were expressed in neural stem cells as well as E12 and E16 telencephalon.

To dissect the VIP signaling pathway during the intense proliferative period of neural progenitors, we studied proliferation of neurosphere-derived progenitors with a BrdU incorporation assay (see Methods) in the presence of VIP, VIP agonists, VA, and activators or inhibitors of the cAMP/PKA pathway. As shown in Figure 4, B and C, VIP stimulated the proliferation of progenitors in a dose-dependent manner and with a classical bell-shaped curve (54), and its maximal effect on BrdU incorporation was completely abolished in the presence of VA. VA alone reduced BrdU incorporation (Figure 4D). The proliferative effect of VIP at nanomolar concentration that excluded an effect through PAC1 receptor by definition (55) could be mimicked by both VPAC1 (Figure 4, E and F) and VPAC2 agonists (Figure 4G). Finally, the VIP stimulatory effect was completely abolished by 2 different PKA inhibitors (H89 and KT5920) and mimicked by forskolin (FSK), an adenylate cyclase activator (Figure 4H). Together, these data suggest that VIP-induced proliferative actions are mediated by VPAC receptors positively coupled with a cAMP/PKA signaling pathway and that this pathway is blocked by VA.

VIP blockade leads to in vivo inhibition of Mcph1 expression. To explore a putative crosstalk between VIP signaling and *MCPH*-related genes, we analyzed *Mcph* gene expression in the telencephalon of both VA-treated animals and controls at different stages. RNA samples were extracted from the telencephalon of control and VA-treated embryos between E12 and P0. Quantitative RT-PCR experiments were performed to measure the expression levels of different genes known to be relevant in human microcephaly, namely *MCPH1*, *WDR62*, *CDK5RAP2*, *CEP152*, *ASPM* (commonest cause of MCPH), *CENPJ*, and *STIL*. All of these genes showed a similar ontogenic pattern with a very high expression during neurogenesis and then decreased until birth. However, only *Mcph1* was significantly downregulated in the telencephalon of VA-treated embryos during the normal peak of expression (between E12 and P0 as compared with controls) (Figure 5, A–G). Moreover, this specific effect of VA on *Mcph1* expression was also observed at the protein level as shown by Western blot (Supplemental Figure 2). To further assess the specificity of VA on *Mcph1* and its downstream targets, we carried out similar experiments on E16 embryos after treatment with VIP, VA, or both between E9 and E11 (Figure 5,

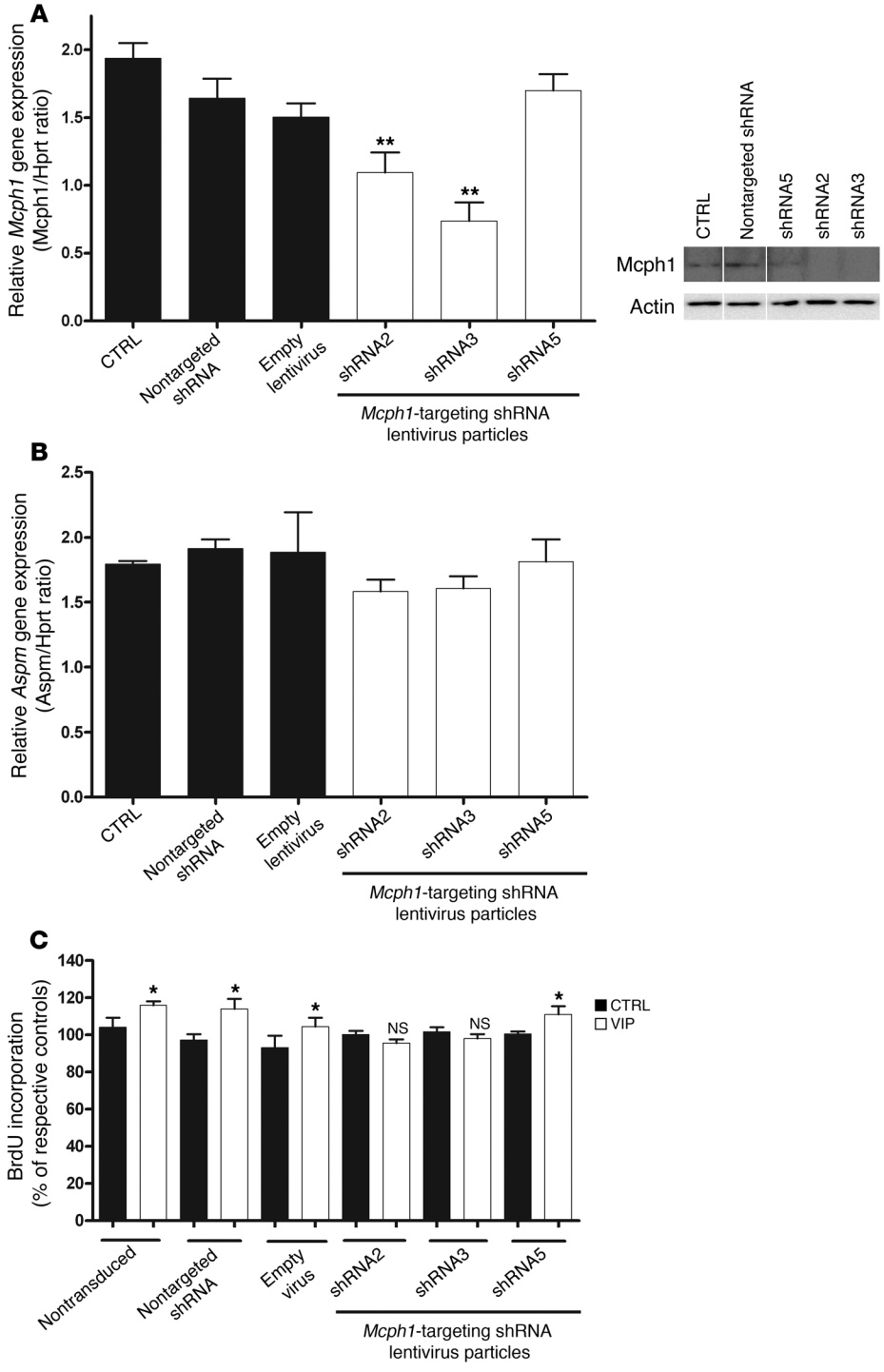

Figure 7

Mcph1 silencing reproduced VA effects on VIP-induced proliferation of neural progenitors. (**A**–**B**) *Mcph1* and *Aspm* gene expression as assessed by quantitative RT-PCR from neurosphere-derived progenitors transduced by *Mcph1*-specific lentiviral-mediated shRNA, *Mcph1*-specific shRNA2, and *Mcph1*-specific shRNA3 specifically inhibits *Mcph1* transcript expression ($n = 3$ per group, 1-way ANOVA, $^{*}P < 0.05$, $^{**}P < 0.01$). The negative controls (empty virus and nontarget shRNA) failed to modulate *Mcph1* expression. Knockdown of *Mcph1* by shRNA2 and shRNA3 results in lost of Mcph1 protein at DIV5 after transduction (**A**, right panel). Knockdown of *Mcph1* fails to affect *Aspm* expression (**B**). (**C**) BrdU incorporation by neurosphere-derived progenitors treated by *Mcph1*-specific shRNA in the presence of VIP or PBS (control). Note that *Mcph1* shRNA2 and shRNA3 abolish VIP-induced proliferation.

H and I). While VA reduced the basal level of expression of *Mcph1*, as expected, VIP had the opposite effect. Interestingly, VIP was able to rescue the VA-induced inhibition of *Mcph1* (Figure 5H), while *Aspm*, used as a negative control, remained unchanged (Figure 5I). In situ hybridization performed at E12.5 showed that, in control embryos, *Mcph1* was expressed along the whole telencephalon in almost all cells of the neuroepithelium (Supplemental Figure 3). In contrast, in VA-treated embryos, *Mcph1* expression was restricted to the outer part of the neuroepithelium of the rostral telencephalon (Supplemental Figure 3). Taken together, these data demonstrate that VIP blockade during neurogenesis specifically reduces the expression of *Mcph1* in embryo telencephalon.

VA acts through VPAC1 receptors to block Mcph1 expression in neurosphere-derived progenitors. To further decipher the signaling pathway triggered by the VIP in our model, we used an in vitro approach based on neurosphere-derived progenitors. As observed in vivo, VA reduced *Mcph1* expression, VIP stimulated *Mcph1* expression, and this latter effect was blocked by cotreatment with VA (Figure 6). VPAC1 agonist but not VPAC2 agonist mimicked VIP-induced expression of *Mcph1* (Figure 6A) and had no effect on *Aspm* expression (Figure 6B). This suggests that, in the same way as in the in vivo experiments, VA specifically inhibits *Mcph1* through VPAC1 signaling in neurosphere-derived progenitors. In vitro, addition of H89 or KT5720 also resulted in significant reduction in expression levels of *Mcph1*, confirming the involvement of PKA activity in the regulation process (Figure 6C). Again, no effect was observed on *Aspm* expression (Figure 6D).

The effect of VIP on proliferation of neurosphere-derived progenitors is abolished in the absence of Mcph1. To confirm the specificity of VIP effects on *Mcph1* signaling, we next aimed to silence *Mcph1* in neurosphere-derived progenitors. Cells were transduced with lentiviral vectors expressing shRNAs, which, once converted into siRNAs, specifically targeted *Mcph1* mRNA. The expression level of *Mcph1* was analyzed by quantitative PCR and Western blot. Data revealed a signifi-

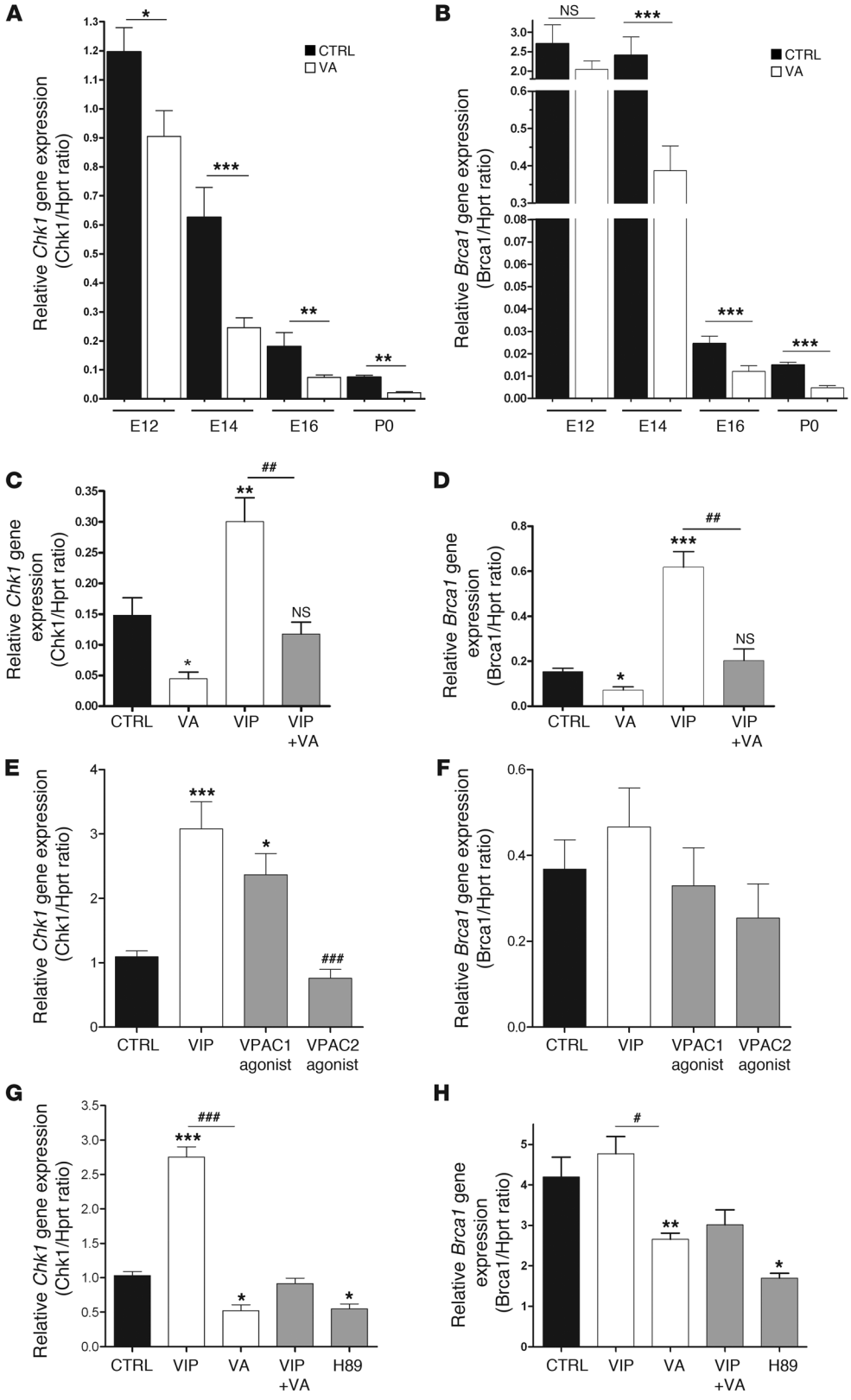

Figure 8

VA treatment reduces *Chk1* and *Brca1* gene expression both in vivo and in vitro. (**A**–**D**) *Chk1* and *Brca1* expression levels assessed by quantitative RT-PCR on RNA samples extracted from telencephalon of embryos (control or VA-treated) from E12 to P0. VA induced a significant decrease in *Chk1* (**A**) and *Brca1* (**B**) expression ($n = 8$ per group, 1-way ANOVA followed by Bonferroni's post-test, $^{*}P < 0.05$, $^{**}P < 0.01$, or $^{***}P < 0.001$). In rescue experiments performed at E16 by quantitative RT-PCR, VIP upregulates both *Chk1* and *Brca1*, while coinjection of VA and VIP significantly represses VIP-induced overexpression of both genes (at $^{\#}P < 0.05$, $^{\#\#}P < 0.01$, or $^{\#\#\#}P < 0.001$) (**C** and **D**). (**E**–**H**) *Chk1* and *Brca1* expression levels in neurosphere-derived progenitors. *Chk1* is upregulated by VIP and blocked by VA (**E** and **G**). VPAC1 agonist increases *Chk1* transcript level, whereas VPAC2 agonist has no effect (**E**). VIP mildly increases *Brca1* gene expression (**F** and **H**), while VA significantly reduces *Brca1* gene expression. H89 inhibits both *Chk1* and *Brca1* gene expression (**G** and **H**), mimicking VA effects.

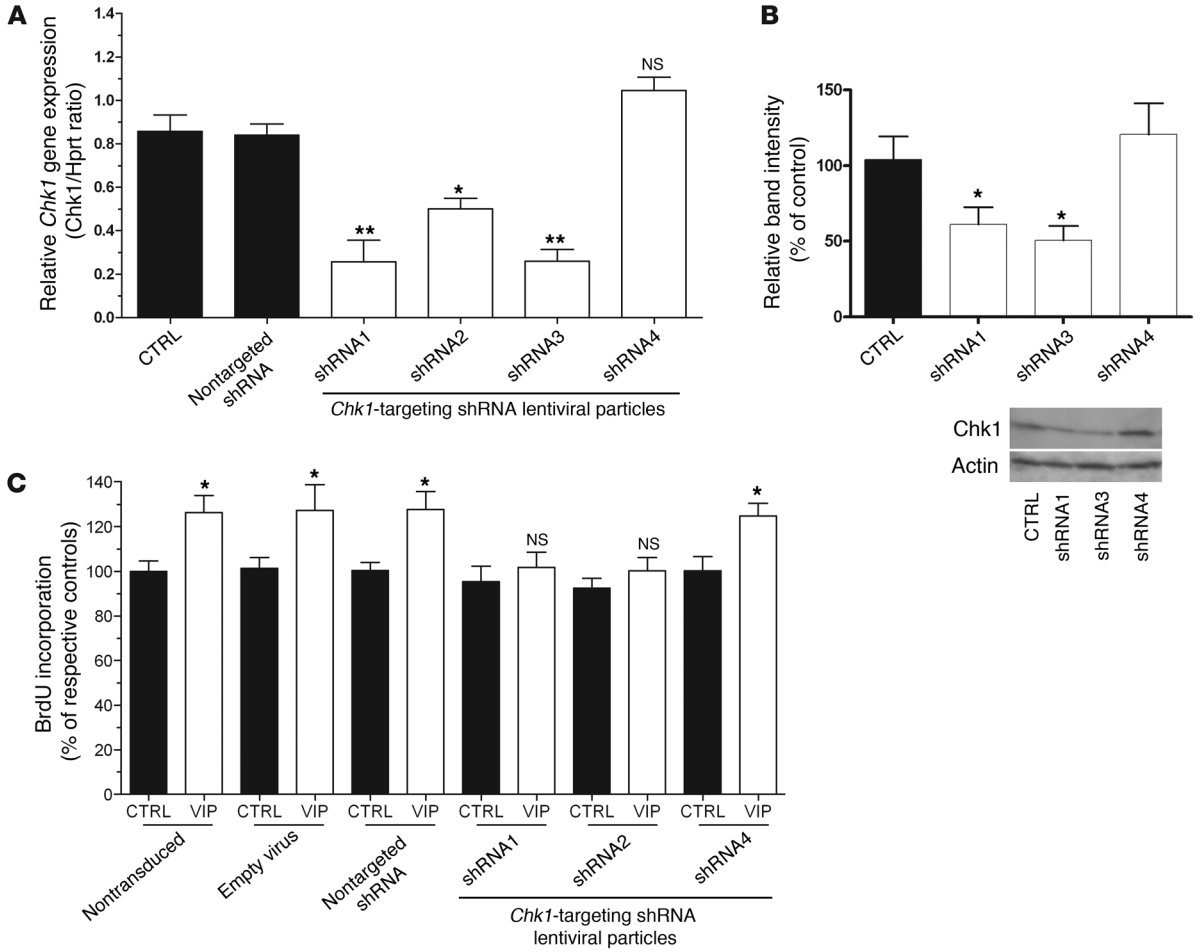

Figure 9

The effects of VIP on neurosphere proliferation are abolished in the absence of *Chk1*. (**A** and **B**) *Chk1* expression levels assessed by quantitative RT-PCR on extracts from neurosphere-derived progenitors transduced by lentiviral-mediated–specific *Chk1*-specific shRNA. Knockdown of *Chk1* gene expression by sequences shRNA1, shRNA2, and shRNA3 significantly reduces both mRNA levels (**A**) and protein contents (**B**), while sequence shRNA4 failed to induce any significant silencing. (**C**) BrdU incorporation in neurosphere-derived progenitors transduced by different control lentiviral vectors and the specific *Chk1* shRNA1 and shRNA 2. Silencing the *Chk1* gene obliterates VIP-induced mitogenic action in neurosphere-derived progenitors. (**A**) $n = 3$ per group, 1-way ANOVA, $^{*}P < 0.05$; $^{**}P < 0.01$. (**B**) $n = 3$ per group, unpaired t test. (**C**) $n = 8$ per group, unpaired t test.

cant inhibition of *Mcph1* expression by 2 separate *Mcph1*-targeting shRNAs (Figure 7A). This selective downregulation of *Mcph1* failed to trigger any effect on *Aspm*, used as a negative control (Figure 7B). Importantly, stimulation of cell growth by VIP was abolished by the selective *Mcph1*-targeting shRNAs (Figure 7C) suggesting that *Mcph1* is required to mediate the effects of VIP on neurogenesis.

VA inhibits Mcph1-Chk1 signaling both in vivo and in vitro. It has been shown that *MCPH1* regulates *CHK1* and *BRCA1* expression (14, 15). *CHK1* and *BRCA1* are involved in DNA repair and cell cycle check point control (56–59) and also play a role in proliferation of undamaged cells (22, 25, 56, 60–62). However, their roles in neurogenesis have not been investigated.

Before addressing the impact of VIP and VA on the expression of *Chk1* and *Brca1*, we confirmed that in neurosphere-derived progenitors, *Mcph1* regulates *Chk1* and *Brca1* expression, using *Mcph1*-targeting shRNAs (Supplemental Figure 4).

To determine whether *Mcph1* targets are regulated by VIP, we studied *Chk1* and *Brca1* expression in the telencephalon of VA-treated embryos and in neurosphere-derived progenitors by quantitative PCR and Western blot. Expression of *Chk1* and *Brca1* genes was found to be decreased by in vivo VA treatment (Figure 8, A and B). Western blot analysis of VA-treated embryos confirmed the significant reduction of Chk1 and showed a similar trend for Brca1 (Supplemental Figure 5). VIP increased in vivo *Chk1* and *Brca1* expression and was able to rescue VA-induced inhibition of *Chk1* and *Brca1* (Figure 8, C and D). In line with the in vivo data, VIP significantly increased *Chk1* expression in neurosphere-derived progenitors (Figure 8E). Its effects on *Chk1* expression were mimicked by a VPAC1 agonist but not by a VPAC2 agonist (Figure 8E). VA inhibited *Chk1* expression, and this effect was mimicked by H89 (Figure 8G). Although it did not reach significance, there was a trend toward an increased expression of *Brca1* following VIP treatment of neurosphere-derived progenitors (Figure 8H). VA significantly inhibited *Brca1* expression, and this effect was mimicked by H89 (Figure 8H). Together, these data indicate that VA inhibits Mcph1-Chk1-Brca1 signaling both in vivo and in vitro through the VPAC1/PKA signaling pathway.

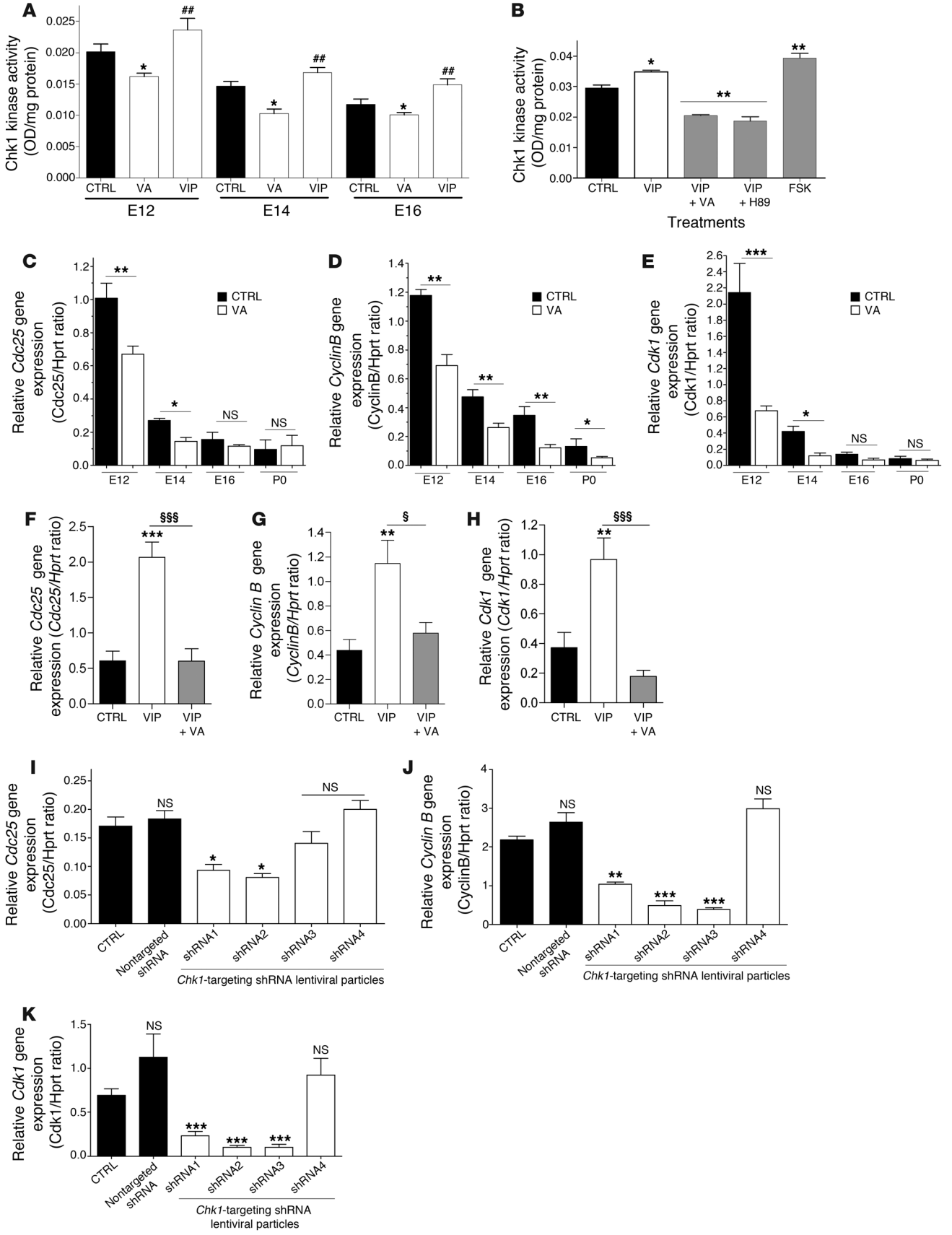
A
Chk1 kinase activity (OD/mg protein)
CTRL
VA
VIP
E12
E14
E16
B
Chk1 kinase activity (OD/mg protein)
CTRL
VIP
VIP + VA
VIP + H89
FSK
Treatments
C
Relative Cdc25 gene expression (Cdc25/Hprt ratio)
CTRL
VA
E12
E14
E16
P0
NS
D
Relative CyclinB gene expression (CyclinB/Hprt ratio)
E
Relative Cdk1 gene expression (Cdk1/Hprt ratio)
F
Relative Cdc25 gene expression (Cdc25/Hprt ratio)
G
Relative Cyclin B gene expression (CyclinB/Hprt ratio)
H
Relative Cdk1 gene expression (Cdk1/Hprt ratio)
I
Relative Cdc25 gene expression (Cdc25/Hprt ratio)
Nontargeted shRNA
shRNA1
shRNA2
shRNA3
shRNA4
Chk1-targeting shRNA lentiviral particles
J
Relative Cyclin B gene expression (CyclinB/Hprt ratio)
K
Relative Cdk1 gene expression (Cdk1/Hprt ratio)
Chk1-targeting shRNA lentiviral particles

Figure 10
Chk1 kinase activity and expression of key cell cycle regulators downstream of *Chk1* are reduced by VA. (**A**) Chk1 kinase activity assessed by kinase essay on telencephalon or cortical extracts from E12 to P0 embryos and newborns that received VA, VIP, or both treatments. At the 3 embryonic ages, Chk1 kinase activity (mean ± SEM) follows the same time-dependent decrease in controls. VIP treatment stimulates Chk1 activity ($n = 5$ per group, run in duplicate, 1-way ANOVA, $^{\#\#}P < 0.01$), while VA suppresses it ($^{*}P < 0.05$, $^{**}P < 0.01$, or $^{***}P < 0.001$). (**B**) Chk1 kinase activity on protein extracts isolated from neurosphere cultures after treatment with VIP or VIP plus VA or cAMP/PKA agents. VIP stimulates kinase activity in neurospheres; such an enhancement was counterbalanced by cotreatment VIP plus VA. H89 inhibited the kinase activity ($^{**}P < 0.01$), while FSK enhanced it. (**C**–**E**) Transcription levels of specific key cell cycle regulators downstream of *Chk1* (*Cdc25*, *cyclin A*/*B Cdk1*, and *Cdk2* genes) assessed by quantitative RT-PCR. Only *Cdc25*, *Cyclin B*, and *Cdk1* transcripts are significantly repressed ($n = 8$, 1-way ANOVA) by VA treatment, but no change is seen in *Cdk2* and *Cyclin A* levels (not shown). (**F**–**H**) Similar experiments conducted in neurosphere-derived progenitors. VIP upregulates *Cdc25* (**F**) *Cyclin B* (**G**), and *Cdk1* (**H**) expression; this effect was inhibited by VA treatment. (**I**–**K**) Efficient *Chk1* targeting by lentiviral-mediated vectors expressing shRNAs (1, -2, and -3) downregulated *Cdc25* (**I**), *cyclin B* (**J**), and *Cdk1* (**K**) expression ($n = 3$, run in duplicate, 1-way ANOVA).

Chk1 is required for VIP proliferative effects on neurosphere-derived progenitors. To assess whether *Chk1* is also necessary to mediate the effect of VIP, we knocked down the expression of *Chk1* in neurospheres. Neurospheres were transduced with lentiviral vectors expressing various shRNAs, which, once converted into siRNAs, specifically targeted *Chk1* mRNA. *Chk1* downregulation was checked by quantitative PCR and Western blot (Figure 9, A and B) and showed that, out of 4 different vectors, only the shRNA4 lentiviral vector failed to inhibit *Chk1* expression. BrdU incorporation experiments were carried out to evaluate VIP effects on neurosphere proliferation (Figure 9C) in the lentiviral-transduced cells. As shown in Figure 9C, VIP failed to stimulate proliferation in *Chk1*-shRNA1– and *Chk1*-shRNA2–transduced cells but was still able to induce that of cells containing the control sequence or *Chk1*-shRNA4 (used here as a negative control). These data indicate that *Chk1* is required for VIP mitotic effects on neurosphere-derived progenitor proliferation.

VIP blockade interferes with cell cycle by modulating Chk1 functions. To determine whether VA affects Chk1 function in addition to *Chk1* expression, we assessed Chk1 kinase activity in vivo (in forebrain/telencephalon from control and VIP- and VA-treated embryos between E12 and P0) and in vitro (in neurosphere-derived progenitors treated by PBS, VIP, or VIP plus VA). At each stage in vivo (Figure 10A) and in neurosphere-derived progenitors (Figure 10B), Chk1 kinase activity was strongly reduced in the presence of VA and strongly enhanced upon VIP stimulation. As expected, H89 blocked VIP effect, thus mimicking VA action, while FSK mirrored VIP activity in vitro (Figure 10B). These data indicate that VIP blockade affects Chk1 function, most likely by modulating the cAMP/PKA pathway.

To determine whether key checkpoints of cell cycle known to be targets of *Chk1* were also affected in our model, we analyzed the expression of cell division cycle 25C (*Cdc25*), *Cyclin B*, and cyclin-dependent kinase 1 (*Cdk1*) (involved in regulation of G_2/M transition) and *Cyclin A* and *Cdk2* (regulation of S phase) by quantitative PCR. As shown in Figure 10, C–E, VA treatment resulted in a strong decrease of *Cdc25*, *cyclin B*, and *Cdk1* expression in vivo. The in vitro approach accordingly showed that VA completely abolishes the effects of VIP on the expression of these genes (Figure 10, F–H). In contrast, expression of *Cdk2* and *Cyclin A* remained unchanged both in vivo and in vitro (data not shown). These data indicate that VIP blockade affects specific cell cycle checkpoints and suggest that VIP blockade has an impact on the G_2/M transition.

To determine whether this effect was mediated by *Chk1*, we analyzed the expression of these G_2/M transition checkpoints following downregulation of *Chk1* expression through the lentiviral-mediated RNA interference approach using the shRNAs specifically directed against *Chk1*. Downregulation of *Chk1* resulted in a reduced expression of *Cdc25*, *Cyclin B*, and *Cdk1* expression, indicating that the effect observed upon VA treatment was mediated by *Chk1* (Figure 10, I–K).

Taken together, these data indicate that VIP blockade interferes with the cell cycle by affecting Chk1 activity and the subsequent modulation of targets involved in G_2/M transition.

Discussion

The basis of the high degree of encephalization in humans is not understood. Discovery of the microcephaly locus was an important step in this process, as it offered an insight into a set of loci that controlled cortical size without an adverse effect on cortical patterning. Interestingly, evolutionary studies do not seem to support the hypothesis that these loci then must have been positively selected for during vertebrate evolution. In this context, there are several external factors that also lead to a large variation in cortical size. Therefore one possible reason for a lack of evidence for the strong positive selection in the MCPH loci is that the high degree of encephalization during evolution is the result of a combination of environmental factors that modulate these genetic loci and therefore the genetic loci itself is but only half the story. To date there has been no evidence linking environmental factors to genes that have been shown to play a role in regulating cortical size, and this is a subject of speculation. In this study, we show for what we believe is the first time that a maternal factor, VIP, modulates MCPH genetic loci that have been associated with cortical expansion and thus points to a mechanism by which a combination of genetic selection and maternal factors may play a role in regulating cortical size.

The most salient feature of the present study is the demonstration that, in mice, VIP blockade–induced microcephaly involves *Mcph1* downregulation, linking a maternal factor to the molecular machinery, which controls the proliferation of neural cell precursors. In addition, in this model, interfering with the expression and/or function of *Chk1*, a known target of *Mcph1*, appears as a key mechanism for the VA-induced blockade of the cell cycle. Finally, VIP blockade slows down proliferation of VZ progenitors through lengthening of cell cycle duration and acceleration of cell cycle exit and progenitor differentiation.

Is the VA-induced microcephaly a relevant model for human MCPH? Several lines of evidence support that the present model mimics different key aspects of human MCPH. Indeed, blockade of VIP signaling during neurogenesis induces a reduction in brain weight, in cortical thickness, and in cortical surface, these anomalies being reminiscent of the cortical phenotype observed in patients with MCPH. In addition, VIP blockade induces the inhibition of expression of the *Mcph1* gene, 1 of the 7 known genes implicated in

MCPH. In contrast, the expression of the other known *Mcph* genes is not affected by VA, supporting the specificity of the effects. Therefore, we believe that the VA model is the first that is relevant for *MCPH1*-related human microcephalies.

How does VIP regulate Mcph1 expression? Pharmacological and mRNA expression data support the hypothesis that VA effects in cell cycle and brain growth are mediated through VPAC1 receptors expressed on NSC progenitors. In agreement with this hypothesis, *VPAC1* mRNA is highly expressed in the VZ of E14 rat embryos (63). As classically described for VPAC1 receptors (64), the transduction pathway implicated in VA effects involves the cAMP/PKA pathway, as demonstrated by the use of H89 and FSK. When activated, cAMP-dependent protein kinase A releases its catalytic subunits, which translocate to the nucleus and induce cellular gene expression by phosphorylating CREB (65). CREB then mediates the activation of cAMP-responsive genes by binding as a dimer to a conserved cAMP-responsive element (CRE), TGACGTCA (66–68). Of interest, the search for such TGACGTCA palindromic octamers in 50 kb of genomic DNA upstream of all 7 mouse *Mcph* genes revealed the presence of 3 distinct CRE sequences in *Mcph1* (located at 15.2 kb, 19.6 kb, and 37 kb upstream of the first exon), 1 CRE sequence in *Wdr62* (located at 15 kb upstream of the first exon), and 1 CRE sequence in *Cep152* (4.88 kb upstream of the first exon), but failed to reveal any CRE sequence upstream of *Cdk5rap2*, *Aspm*, *Cenpj*, and *Stil*. These findings support the idea that the specific *Mcph1* regulation by VIP involves the cAMP/PKA pathway. We cannot exclude that other transduction pathways are involved in VIP effects since (a) VIP has been shown to activate other pathways including PKC and MAPK pathways (69), and (b) our preliminary screen of transduction inhibitors showed that PKC blockade, but not MAPK blockade, partially reversed VIP effects (data not shown).

How does Mcph1 downregulation lead to blockade of neural cell proliferation? MCPH1 has been shown to regulate the expression of *CHK1* and *BRCA1* (14, 15). In the present study, inhibition of *Mcph1*, through VA or direct gene silencing, induced a downregulation of *Chk1* and *Brca1* in neural progenitors both in vivo and in vitro. Since the effects of VA and *Mcph1* inhibition on *Chk1* expression were of a larger amplitude than those observed on *Brca1* expression, we focused our study on *Chk1* inhibition and its impact on progenitor proliferation, although future studies will be necessary to determine whether *Brca1* inhibition participates as well in the reduced proliferation observed with VA treatment.

CHK1, when activated through the phosphorylation of several C-terminal residues, displays a kinase activity, inducing phosphorylation of numerous downstream proteins including key cell cycle regulators (58, 59). In addition, more recent data support the hypothesis that CHK1 binds to chromatin and has a direct transcriptional activity (70–72). In terms of biological effects, a large body of literature implicates CHK1 in DNA repair (58, 73). However, more recently, CHK1 has also been shown to regulate the cell cycle of cells with undamaged DNA through a mechanism most likely independent (phosphorylation at a different residue) of DNA repair (22, 25, 60, 61, 74). Indeed, depletion of CHK1 in somatic cells under unperturbed conditions induces S-phase arrest and repression of *CYCLIN B1* and *CDK1* expression (70). Interestingly, *Chk1*$^{-/-}$ mice die at E6.5, further supporting a role of Chk1 during normal embryonic development (75). In the present study, we provide experimental data supporting the hypothesis that downregulation of *Chk1* is sufficient to slow down the proliferation of neural progenitors. The underlying mechanism could involve phosphorylation of proteins controlling the mitotic cycle through Chk1 kinase activity and/or transcription of genes controlling cell cycle progression such as the cyclin-dependent cyclin *Cdc25* and *cyclin B* and the cyclin-dependent kinase *Cdk1*. Of interest, in agreement with previous studies showing that CHK1 depletion induces S phase (70), the present study shows that VA treatment induces S-phase lengthening of VZ neural progenitors.

What are the clinical implications of the modulation of neural cell proliferation by a maternal factor? In neural progenitors, the cell cycle is regulated in a tight, specific, and timely manner (for review, see ref. 76) and the molecular mechanisms underlying this control seem to be largely conserved through evolution of mammals (77–79).

VIP has previously been shown to be a maternal factor acting on early brain development in rodents (80). Similarly, some data also suggest that maternal VIP could act on the embryonic and fetal brain in humans (41). Here, we demonstrate that administration of VA to pregnant mice during neurogenesis induces embryonic microcephaly with as much as 20% reduction of overall cortical thickness. This VA effect is mediated through the regulation of the expression and/or function of *Mcph1* and *Chk1*, which are important regulators of the cell cycle. Our data strongly suggest that environmental factors, including maternal ones, can influence the tightly controlled molecular machinery of neural progenitor proliferation. Comparable modulation of this intrinsic molecular machinery has been described for irradiation that induces murine microcephaly through *Aspm* gene inhibition (81). Together, these data raise the hypothesis that other environmental factors could impinge on the intrinsic control of neural progenitor proliferation and therefore modulate the final size of the brain.

Methods

Animals. All animal experiments were carried out according to protocols approved by the institutional review committee (Bichat-Robert Debré Ethical Committee, Paris, France) and meet stipulations of the Guide for the Care and Use of Laboratory Animals (NIH, Bethesda, Maryland, USA). All experiments were performed in Swiss mice (Elevage Janvier).

The day of vaginal plug was considered E0.5. Pregnant mice were killed by cervical dislocation. Embryos were harvested in cold PBS and fixed overnight in freshly prepared 4% PFA. For immunohistochemistry, they were then either dehydrated in ascending grades of ethanol and embedded in paraffin or cryoprotected in 10% sucrose overnight and embedded in 7.5% gelatin/10% sucrose solution prior to flash freezing in isopentane. Tissues were later cut sagitally at 10 μm on cryostat or coronally at 7 μm on microtome. Newborn and adult animals were anesthetized with isoflurane and intracardiacally perfused with a 0.9% NaCl solution followed by 4% PFA. Brains were dissected and postfixed either overnight in 4% PFA and cryopreserved in gelatin/sucrose or in 4% formol for 4 days prior to embedding in paraffin. For in situ hybridization, embryos were fixed in 4% PFA overnight, then cryoprotected in 30% sucrose overnight and embedded in 7.5% gelatin/30% sucrose solution, frozen in isopentane, and cut coronally at 10 μm. In situ hybridization was performed according to Ravassard et al. (82) using a digoxigenin-labeled RNA antisense probe corresponding to nt 1-1146 of *Mcph1*.

Animal injections. Pregnant Swiss mice were injected intraperitoneally twice a day (8–9 am and 6–7 pm) between E9.5 and E11.5 with 50 μl of either PBS (vehicle) or VA (hybrid of VIP and neurotensin, which is a competitive antagonist of VIP receptors (83), or again VIP, according to the original protocol designed by Gressens et al. (43, 44). Both peptides were purchased from Bachem and injected at the final concentration of 2 μg/g body weight.

Cell cycle study, BrdU, and IdU injections. On E11.5, IdU was injected 1 hour after the latest VA injection into pregnant females followed by BrdU injections (50 mg/g body weight each) performed 90 minutes later. Dams were sacrificed 2 hours after the IdU injection according to the original protocol schematically depicted on Figure 2C. Embryos were fixed with 4% PFA, cut (10 μm cryostat sections), and processed for double immunostaining (see below). Sections were immunolabeled with monoclonal anti-BrdU antibodies raised in mouse or rat that recognized either the 2 analogs or BrdU alone, respectively.

Histology, immunohistochemistry. Histopathological features of embryonic telencephalon or brains were studied by analyzing E11.5, E12.5, and P5 control or treated Swiss mice. Tissues were processed for histology and immunohistochemistry as described in Supplemental Methods. BrdU and p27kip1 antibodies were from BD, BrdU and Dcx antibodies from Abcam, Calretinin and Calbindin antibodies from Swant, NeuN antibodies from Chemicon, GFAP antibody from Dako, cleaved caspase-3 antibody from Cell Signaling, Cux1 antibody from Santa Cruz Biotechnology Inc., Satb2 and Tbr1 antibodies from Abcam. TUNEL was performed using the In Situ Cell Death Detection Kit, Fluorescein, from Roche.

Quantifications. Quantification of cortical thickness, surface, and NeuN stainings was performed on primary somatosensory cortex (S1) (see Supplemental Methods). Quantification of DAPI, BrdU-IdU C–Caspase-3 and p27kip1 (at E11.5) and Dcx and Calretinin (at E12.5) staining were performed on images from the dorsal telencephalon (see Supplemental Methods). For all quantifications, the embryos and brains (6 to 8 per group) were taken from at least 2 litters.

Neurosphere-derived progenitor culture. Primary neural stem cell cultures or neurospheres were established from the forebrain of embryos at gestation E10.5 using trypsin dissociation as described in Supplemental Methods.

Drug administration was performed at 3 days in vitro after the first passage of neurospheres. Neural stem cells were harvested at 4 and 20 hours after treatment for BrdU experiments and RNA extraction, respectively. Peptides including VIP, VA, VPAC1 agonist ($VIP_{[A11A22A28]}$) (64), and VPAC2 agonist ($VIP_{[A19K27K28]}$) (84) were used at final concentrations ranging from 10 pM to 1 μM, while signaling modulators such as H-89 and FSK (Calbiochem) were used at 20 and 30 μM, respectively.

Cell proliferation studies. BrdU incorporation assay (Cell Proliferation Kit; Roche) was performed on neurosphere-derived progenitors according to the manufacturer's instructions as described in Supplemental Methods.

Western blot. Freshly excised cortices were soaked into cell lysis buffer purchased from Cell Signaling and supplemented with protease inhibitors including 1 mM sodium orthovanadate, 1 μg/ml leupeptin, and 10 μM PMSF. Total proteins, 20 or 60 μg /lane, for cell and tissue extracts, respectively, were loaded onto 12% SDS-polyacrylamide gels and transferred to nitrocellulose membranes (GE Healthcare). Membranes were probed with mouse anti-actin (1/10,000; Chemicon), anti-BRCA1 (1/200; Chemicon), rabbit anti-MCPH1 (1/500; Abcam), anti-CDK5RAP2 (1/2000; Bethyl), anti-ASPM (1/200; Novus), anti-CENPJ (1/800; Abcam), anti-STIL (1/500;, Abcam), and goat anti-CHK1 (1/1,000; R&D) antibodies. Antibodies were revealed by horseradish peroxidase–coupled conjugates, and the staining intensity was analyzed with the ImageJ program (NIH).

RNA extraction and relative quantification of gene expression by real-time PCR. Samples were isolated from animals aged from E12 to P40. Forebrains and cortices were dissected and total RNA was extracted as previously described (85). After RT was performed using iScript cDNA kit (Bio-Rad), real-time RT-PCR were performed as described elsewhere (86). Primer sequences are listed in Supplemental Table 2.

Kinase assay. Chk1 kinase assay was performed on telencephalon or cortice extracts or neurosphere-derived progenitors using Active Chk1 Kinase IP-Kinase Assay (DuoSet IC; R&D Systems) as described in Supplemental Methods.

Lentiviral transduction. A set of 3 lentiviral vectors carrying different shRNAs targeting *Mcph1* and 4 lentiviral vectors carrying different shRNAs targeting *Chk1* was purchased from Sigma-Aldrich. They were provided as ready-to-use lentiviral particles. The shRNA corresponding sequences are given in Supplemental Table 3. Neurosphere-derived progenitors were transduced by lentiviral particles according to manufacturer recommendations as described in Supplemental Methods.

Statistics. Quantitative data are expressed as mean ± SEM for each treatment group. Results were compared using Student's *t* tests (2-tailed) or ANOVA with Bonferroni's multiple comparison of means test (GraphPad Prism; GraphPad Software). $P < 0.05$ was considered significant.

Acknowledgments

This work was supported by Inserm, CNRS, the Université Paris Diderot, the Université de Strasbourg, Assistance Publique Hôpitaux de Paris (APHP) (Contrat d'Interface to P. Gressens), the Fondation Lejeune, the Fondation Grace de Monaco, the Fondation pour la Recherche Médicale, the Société Française de Neuropédiatrie, the Journées de Neurologie de Langue Française, and Indo French Centre for the Promotion of Advanced Research–Centre Indo-Français Pour la Recherche Avancée (IFCPAR-CEFIPRA) (project number 3803-3 to S. Mani and P. Gressens).

Received for publication May 25, 2010, and accepted in revised form May 11, 2011.

Address correspondence to: Pierre Gressens, Inserm U676, Hôpital Robert Debré, 48 Blvd Serurier, F-75019 Paris, France. Phone: 33.1.40.03.19.76; Fax: 33.1.40.03.19.95; E-mail: pierre.gressens@inserm.fr. Or to: Vincent Lelièvre, CNRS UPR-3212, 5 rue Blaise Pascal, F-67084 Strasbourg Cedex, France. Phone: 33.3.88.45.66.59; Fax: 33.3.88.60.16.64; E-mail: lelievre@inci-cnrs.unistra.fr.

1. Aicardi J. Malformations of the central nervous system in childhood. In: *Diseases Of The Nervous System In Childhood*. 2nd ed. London, United Kingdom: Mac Keith Press; 1998:90–91.
2. Kaindl AM, Passemard S, Kumar P, Kraemer N, Issa L, Zwirner A, Gerard B, Verloes A, Mani S, Gressens P. Many roads lead to primary autosomal recessive microcephaly. *Prog Neurobiol*. 2010;90(3):363–83.
3. Passemard S, Kaindl AM, Titomanlio L, Gerard B, Gressens P, Verloes A. Primary Autosomal Recessive Microcephaly. In: Pagon RA, et al., eds. GeneReviews. Medical Genetics Information Resource [database online]. Seattle, Washington, USA: University of Washington: 1997–2009. NCBI Web site. http://www.ncbi.nlm.nih.gov/sites/GeneTests/review?db=genetests. Accessed May 12, 2011.
4. Jackson AP, et al. Identification of microcephalin, a protein implicated in determining the size of the human brain. *Am J Hum Genet*. 2002;71(1):136–142.
5. Bilguvar K, et al. Whole-exome sequencing identifies recessive WDR62 mutations in severe brain malformations. *Nature*. 2010;467(7312):207–210.
6. Nicholas AK, et al. WDR62 is associated with the spindle pole and is mutated in human microcephaly. *Nat Genet*. 2010;42(11):1010–1014.
7. Yu TW, et al. Mutations in WDR62, encoding a centrosome-associated protein, cause microcephaly with simplified gyri and abnormal cortical architecture. *Nat Genet*. 2010;42(11):1015–1020.
8. Bond J, et al. A centrosomal mechanism involving CDK5RAP2 and CENPJ controls brain size. *Nat Genet*. 2005;37(4):353–355.
9. Guernsey DL, et al. Mutations in centrosomal protein CEP152 in primary microcephaly families linked to MCPH4. *Am J Hum Genet*. 2010;87(1):40–51.
10. Bond J, et al. ASPM is a major determinant of cerebral cortical size. *Nat Genet*. 2002;32(2):316–320.
11. Kumar A, Girimaji SC, Duvvari MR, Blanton SH. Mutations in STIL, encoding a pericentriolar and centrosomal protein, cause primary microcephaly. *Am J Hum Genet*. 2009;84(2):286–290.
12. Alderton GK, et al. Regulation of mitotic entry by microcephalin and its overlap with ATR signalling. *Nat Cell Biol*. 2006;8(7):725–733.
13. Erez A, et al. The mitotic checkpoint gene, SIL is regulated by E2F1. *Int J Cancer*. 2008;123(7):1721–1725.
14. Lin SY, Rai R, Li K, Xu ZX, Elledge SJ. BRIT1/MCPH1 is a DNA damage responsive protein that regulates the Brca1-Chk1 pathway, implicating checkpoint dysfunction in microcephaly. *Proc Natl Acad Sci U S A*. 2005;102(42):15105–15109.

15. Xu X, Lee J, Stern DF. Microcephalin is a DNA damage response protein involved in regulation of CHK1 and BRCA1. *J Biol Chem*. 2004;279(33):34091–34094.
16. Pfaff KL, Straub CT, Chiang K, Bear DM, Zhou Y, Zon LI. The zebra fish cassiopeia mutant reveals that SIL is required for mitotic spindle organization. *Mol Cell Biol*. 2007;27(16):5887–5897.
17. Zhong X, Liu L, Zhao A, Pfeifer GP, Xu X. The abnormal spindle-like, microcephaly-associated (ASPM) gene encodes a centrosomal protein. *Cell Cycle*. 2005;4(9):1227–1229.
18. Zhong X, Pfeifer GP, Xu X. Microcephalin encodes a centrosomal protein. *Cell Cycle*. 2006;5(4):457–458.
19. Gowen LC, Johnson BL, Latour AM, Sulik KK, Koller BH. Brca1 deficiency results in early embryonic lethality characterized by neuroepithelial abnormalities. *Nat Genet*. 1996;12(2):191–194.
20. Kalay E, et al. CEP152 is a genome maintenance protein disrupted in Seckel syndrome. *Nat Genet*. 2010;43(1):23–26.
21. Kramer A, et al. Centrosome-associated Chk1 prevents premature activation of cyclin-B-Cdk1 kinase. *Nat Cell Biol*. 2004;6(9):884–891.
22. Loffler H, Rebacz B, Ho AD, Lukas J, Bartek J, Kramer A. Chk1-dependent regulation of Cdc25B functions to coordinate mitotic events. *Cell Cycle*. 2006;5(21):2543–2547.
23. Rai R, et al. BRIT1 regulates early DNA damage response, chromosomal integrity, and cancer. *Cancer Cell*. 2006;10(2):145–157.
24. Rai R, et al. Differential regulation of centrosome integrity by DNA damage response proteins. *Cell Cycle*. 2008;7(14):2225–2233.
25. Tang J, Erikson RL, Liu X. Checkpoint kinase 1 (Chk1) is required for mitotic progression through negative regulation of polo-like kinase 1 (Plk1). *Proc Natl Acad Sci U S A*. 2006;103(32):11964–11969.
26. Izraeli S, et al. The SIL gene is required for mouse embryonic axial development and left-right specification. *Nature*. 1999;399(6737):691–694.
27. Lam MH, Liu Q, Elledge SJ, Rosen JM. Chk1 is haploinsufficient for multiple functions critical to tumor suppression. *Cancer Cell*. 2004;6(1):45–59.
28. Liang Y, et al. BRIT1/MCPH1 is essential for mitotic and meiotic recombination DNA repair and maintaining genomic stability in mice. *PLoS Genet*. 2010;6(1):e1000826.
29. Trimborn M, et al. Establishment of a Mouse Model with Misregulated Chromosome Condensation due to Defective Mcph1 Function. *PLoS One*. 2010; 5(2):e9242.
30. Feng Y, Walsh CA. Mitotic spindle regulation by Nde1 controls cerebral cortical size. *Neuron*. 2004; 44(2):279–293.
31. Cuzon VC, Yeh PW, Yanagawa Y, Obata K, Yeh HH. Ethanol consumption during early pregnancy alters the disposition of tangentially migrating GABAergic interneurons in the fetal cortex. *J Neurosci*. 2008;28(8):1854–1864.
32. Marret S, Gressens P, Van–Maele–Fabry G, Picard J, Evrard P. Caffeine–induced disturbances of early neurogenesis in whole mouse embryo cultures. *Brain Res*. 1997;773(1–2):213–216.
33. Sadraie SH, et al. Effects of maternal oral administration of morphine sulfate on developing rat fetal cerebrum: a morphometrical evaluation. *Brain Res*. 2008;1245:36–40.
34. Sargeant TJ, Day DJ, Miller JH, Steel RW. Acute in utero morphine exposure slows G2/M phase transition in radial glial and basal progenitor cells in the dorsal telencephalon of the E15.5 embryonic mouse. *Eur J Neurosci*. 2008;28(6):1060–1067.
35. Takano T, Akahori S, Takeuchi Y, Ohno M. Neuronal apoptosis and gray matter heterotopia in microcephaly produced by cytosine arabinoside in mice. *Brain Res*. 2006;1089(1):55–66.
36. Griffith E, et al. Mutations in pericentrin cause Seckel syndrome with defective ATR-dependent DNA damage signaling. *Nat Genet*. 2008;40(2):232–236.
37. Cote F, et al. Maternal serotonin is crucial for murine embryonic development. *Proc Natl Acad Sci U S A*. 2007;104(1):329–334.
38. Mairet-Coello G, Tury A, DiCicco-Bloom E. Insulin-like growth factor-1 promotes G(1)/S cell cycle progression through bidirectional regulation of cyclins and cyclin-dependent kinase inhibitors via the phosphatidylinositol 3-kinase/Akt pathway in developing rat cerebral cortex. *J Neurosci*. 2009; 29(3):775–788.
39. Sahara S, O'Leary DD. Fgf10 regulates transition period of cortical stem cell differentiation to radial glia controlling generation of neurons and basal progenitors. *Neuron*. 2009;63(1):48–62.
40. Vitalis T, Cases O, Passemard S, Callebert J, Parnavelas JG. Embryonic depletion of serotonin affects cortical development. *Eur J Neurosci*. 2007; 26(2):331–344.
41. Ottesen B, et al. Vasoactive intestinal polypeptide and the female genital tract: relationship to reproductive phase and delivery. *Am J Obstet Gynecol*. 1982; 143(4):414–420.
42. Spong CY, et al. Maternal regulation of embryonic growth: the role of vasoactive intestinal peptide. *Endocrinology*. 1999;140(2):917–924.
43. Gressens P, Hill JM, Gozes I, Fridkin M, Brenneman DE. Growth factor function of vasoactive intestinal peptide in whole cultured mouse embryos. *Nature*. 1993;362(6416):155–158.
44. Gressens P, Hill JM, Paindaveine B, Gozes I, Fridkin M, Brenneman DE. Severe microcephaly induced by blockade of vasoactive intestinal peptide function in the primitive neuroepithelium of the mouse. *J Clin Invest*. 1994;94(5):2020–2027.
45. Gozes I, et al. An antagonist to vasoactive intestinal peptide affects cellular functions in the central nervous system. *J Pharmacol Exp Ther*. 1991; 257(3):959–966.
46. Gozes I, Meltzer E, Rubinrout S, Brenneman DE, Fridkin M. Vasoactive intestinal peptide potentiates sexual behavior: inhibition by novel antagonist. *Endocrinology*. 1989;125(6):2945–2949.
47. Moody TW, et al. A vasoactive intestinal peptide antagonist inhibits non-small cell lung cancer growth. *Proc Natl Acad Sci U S A*. 1993;90(10):4345–4349.
48. Gressens P, Paindaveine B, Hill JM, Evrard P, Brenneman DE. Vasoactive intestinal peptide shortens both G1 and S phases of neural cell cycle in whole postimplantation cultured mouse embryos. *Eur J Neurosci*. 1998;10(5):1734–1742.
49. Martynoga B, Morrison H, Price DJ, Mason JO. Foxg1 is required for specification of ventral telencephalon and region-specific regulation of dorsal telencephalic precursor proliferation and apoptosis. *Dev Biol*. 2005;283(1):113–127.
50. Quinn JC, et al. Pax6 controls cerebral cortical cell number by regulating exit from the cell cycle and specifies cortical cell identity by a cell autonomous mechanism. *Dev Biol*. 2007;302(1):50–65.
51. Takahashi T, Nowakowski RS, Caviness VS Jr. The cell cycle of the pseudostratified ventricular epithelium of the embryonic murine cerebral wall. *J Neurosci*. 1995;15(9):6046–6057.
52. Nguyen L, et al. p27kip1 independently promotes neuronal differentiation and migration in the cerebral cortex. *Genes Dev*. 2006;20(11):1511–1524.
53. Francis F, et al. Doublecortin is a developmentally regulated, microtubule-associated protein expressed in migrating and differentiating neurons. *Neuron*. 1999;23(2):247–256.
54. Brenneman DE, et al. Neuronal cell killing by the envelope protein of HIV and its prevention by vasoactive intestinal peptide. *Nature*. 1988; 335(6191):639–642.
55. Vaudry D, Gonzalez BJ, Basille M, Yon L, Fournier A, Vaudry H. Pituitary adenylate cyclase-activating polypeptide and its receptors: from structure to functions. *Pharmacol Rev*. 2000;52(2):269–324.
56. Huen MS, Sy SM, Chen J. BRCA1 and its toolbox for the maintenance of genome integrity. *Nat Rev Mol Cell Biol*. 2010;11(2):138–148.
57. Mullan PB, Quinn JE, Harkin DP. The role of BRCA1 in transcriptional regulation and cell cycle control. *Oncogene*. 2006;25(43):5854–5863.
58. Reinhardt HC, Yaffe MB. Kinases that control the cell cycle in response to DNA damage: Chk1, Chk2, and MK2. *Curr Opin Cell Biol*. 2009;21(2):245–255.
59. Sancar A, Lindsey-Boltz LA, Unsal-Kacmaz K, Linn S. Molecular mechanisms of mammalian DNA repair and the DNA damage checkpoints. *Annu Rev Biochem*. 2004;73:39–85.
60. Wilsker D, Bunz F. Chk1 phosphorylation during mitosis: a new role for a master regulator. *Cell Cycle*. 2009;8(8):1161–1163.
61. Wilsker D, Petermann E, Helleday T, Bunz F. Essential function of Chk1 can be uncoupled from DNA damage checkpoint and replication control. *Proc Natl Acad Sci U S A*. 2008;105(52):20752–20757.
62. Zachos G, et al. Chk1 is required for spindle checkpoint function. *Dev Cell*. 2007;12(2):247–260.
63. Basille M, et al. Comparative distribution of pituitary adenylate cyclase-activating polypeptide (PACAP) binding sites and PACAP receptor mRNAs in the rat brain during development. *J Comp Neurol*. 2000;425(4):495–509.
64. Laburthe M, Couvineau A, Tan V. Class II G protein-coupled receptors for VIP and PACAP: structure, models of activation and pharmacology. *Peptides*. 2007;28(9):1631–1639.
65. Mayr B, Montminy M. Transcriptional regulation by the phosphorylation-dependent factor CREB. *Nat Rev Mol Cell Biol*. 2001;2(8):599–609.
66. Comb M, Birnberg NC, Seasholtz A, Herbert E, Goodman HM. A cyclic AMP- and phorbol ester-inducible DNA element. *Nature*. 1986;323(6086):353–356.
67. Montminy MR, Sevarino KA, Wagner JA, Mandel G, Goodman RH. Identification of a cyclic-AMP-responsive element within the rat somatostatin gene. *Proc Natl Acad Sci U S A*. 1986;83(18):6682–6686.
68. Short JM, Wynshaw-Boris A, Short HP, Hanson RW. Characterization of the phosphoenolpyruvate carboxykinase (GTP) promoter-regulatory region. II. Identification of cAMP and glucocorticoid regulatory domains. *J Biol Chem*. 1986;261(21):9721–9726.
69. Laburthe M, Couvineau A, Marie JC. VPAC receptors for VIP and PACAP. *Receptors Channels*. 2002; 8(3–4):137–153.
70. Shimada M, et al. Chk1 is a histone H3 threonine 11 kinase that regulates DNA damage-induced transcriptional repression. *Cell*. 2008;132(2):221–232.
71. Smits VA. Spreading the signal: dissociation of Chk1 from chromatin. *Cell Cycle*. 2006;5(10):1039–1043.
72. Smits VA, Reaper PM, Jackson SP. Rapid PIKK-dependent release of Chk1 from chromatin promotes the DNA-damage checkpoint response. *Curr Biol*. 2006;16(2):150–159.
73. Stracker TH, Usui T, Petrini JH. Taking the time to make important decisions: the checkpoint effector kinases Chk1 and Chk2 and the DNA damage response. *DNA Repair (Amst)*. 2009;8(9):1047–1054.
74. Petermann E, Caldecott KW. Evidence that the ATR/Chk1 pathway maintains normal replication fork progression during unperturbed S phase. *Cell Cycle*. 2006;5(19):2203–2209.
75. Liu Q, et al. Chk1 is an essential kinase that is regulated by Atr and required for the G(2)/M DNA damage checkpoint. *Genes Dev*. 2000;14(12):1448–1459.
76. Dehay C, Kennedy H. Cell-cycle control and cortical development. *Nat Rev Neurosci*. 2007;8(6):438–450.
77. Evans PD, Mekel-Bobrov N, Vallender EJ, Hudson RR, Lahn BT. Evidence that the adaptive allele of the brain size gene microcephalin introgressed into Homo sapiens from an archaic Homo lineage. *Proc Natl Acad Sci U S A*. 2006;103(48):18178–18183.
78. Gilbert SL, Dobyns WB, Lahn BT. Genetic links

between brain development and brain evolution. *Nat Rev Genet*. 2005;6(7):581–590.
79. Hill RS, Walsh CA. Molecular insights into human brain evolution. *Nature*. 2005;437(7055):64–67.
80. Hill JM, et al. Maternal vasoactive intestinal peptide and the regulation of embryonic growth in the rodent. *J Clin Invest*. 1996;97(1):202–208.
81. Fujimori A, et al. Ionizing radiation downregulates ASPM, a gene responsible for microcephaly in humans. *Biochem Biophys Res Commun*. 2008; 369(3):953–957.
82. Ravassard P, Chatail F, Mallet J, Icard-Liepkalns C. Relax, a novel rat bHLH transcriptional regulator transiently expressed in the ventricular proliferating zone of the developing central nervous system. *J Neurosci Res*. 1997;48(2):146–158.
83. Gozes Y, Brenneman DE, Fridkin M, Asofsky R, Gozes I. A VIP antagonist distinguishes VIP receptors on spinal cord cells and lymphocytes. *Brain Res*. 1991;540(1–2):319–321.
84. Langer I, Gregoire F, Nachtergael I, De Neef P, Vertongen P, Robberecht P. Hexanoylation of a VPAC2 receptor-preferring ligand markedly increased its selectivity and potency. *Peptides*. 2004;25(2):275–278.
85. Fontaine RH, et al. IL-9/IL-9 receptor signaling selectively protects cortical neurons against developmental apoptosis. *Cell Death Differ*. 2008; 15(10):1542–1552.
86. Favrais G, Couvineau A, Laburthe M, Gressens P, Lelievre V. Involvement of VIP and PACAP in neonatal brain lesions generated by a combined excitotoxic/inflammatory challenge. *Peptides*. 2007; 28(9):1727–1737.